Molecular Phylogenetics and Evolution 225 (2026) 108697

Contents lists available at ScienceDirect

Molecular Phylogenetics and Evolution

journal homepage: www.elsevier.com/locate/ympev

Diversity and population connectivity of members of the family Eunicidae inhabiting deep-water corals in the North Atlantic

Carlota Gracia-Sancha [a,b,*], Nicolai Roterman [c,d], Michelle L. Taylor [e], Kerry L. Howell [f,g], Alex D. Rogers [h], Sofía Ruiz-Cano [b,j], Sergi Taboada [a,i]

[a] Departamento de Biodiversidad y Biología Evolutiva, Museo Nacional de Ciencias Naturales (MNCN), CSIC, 28006 Madrid, Spain
[b] Departamento de Biodiversidad, Ecología y Evolución (BEE), Facultad de Biología, Universidad Complutense de Madrid (UCM), 28040 Madrid, Spain
[c] School of the Environment and Life Sciences, King Henry Building, Portsmouth University, PO1 2UP Portsmouth, United Kingdom
[d] Institute of Marine Science, Portsmouth University, PO1 2UP Portsmouth, United Kingdom
[e] School of Life Sciences, University of Essex CO4 3SQ Essex, United Kingdom
[f] Plymouth Marine Laboratory, Prospect Place, Plymouth, Devon PL1 3DH, United Kingdom
[g] University of Plymouth, Drake Circus, Plymouth, Devon PL48AA, United Kingdom
[h] National Oceanography Centre, Southampton SO14 3ZH, United Kingdom
[i] Department of Life Sciences, Natural History Museum, SW7 5BD London, United Kingdom
[j] Departamento de Biología, Universidad Autónoma de Madrid 28049 Madrid, Spain

ARTICLE INFO

Keywords:
CWCs
Eunicids
Genetic connectivity
Panmictic population
RADseq

ABSTRACT

Eunicid polychaetes are often found in association with Cold Water Corals (CWCs), even establishing symbiotic relationships, such as those described between *Desmophyllum pertusum* and *Eunice norvegica*. While genetic connectivity of CWCs across the North Atlantic has been widely studied, little is known about their associated fauna in this regard. Here, we present a study combining a focused analysis of the genetic and genomic connectivity of *E. norvegica* with a regional assessment of the distribution and evolutionary relationships of three CWC-associated eunicid species from the Cantabrian Sea and the North of the United Kingdom (190–1,230 m depth). An integrative approach using genetic (*16S*, *COI* and *18S*), morphological and ecological data allowed the identification of the eunicids studied, with new records of *Eunice* cf. *nicidioformis* and *Leodice* cf. *antarctica* in the Cantabrian Sea, as well as previously undocumented associations with CWC species. In addition, RADseq data contributed to the delimitation of the closely related species *E. norvegica* and *Eunice philocorallia*. Moreover, the genetic connectivity of *E. norvegica* was studied trough a RADseq (1,067 neutral SNPs) approach. Our results indicate a single panmictic population across approximately 2,000 km, suggesting that oceanographic currents facilitate passive dispersal of *E. norvegica* lecithotrophic larvae, aided by coral host stepping-stones. The connectivity patterns observed for *E. norvegica* mirror those of *D. pertusum*, on which the worm is ecologically dependent. Our study highlights the importance of using integrated genetic, morphological and ecological data to characterise and delineate understudied CWC-associated species and improve our understanding of their dispersal capabilities and genetic connectivity to inform future conservation recommendations.

1. Introduction

Cold Water Corals (CWCs) are abundant in the deep-sea and constitute one of the most significant ecosystem engineers on continental shelves, slopes, canyons, seamounts and ridge systems across the globe (Roberts et al., 2009; Cairns, 2007). Reef structures formed by CWCs offer key ecosystem services including nutrient recycling, and providing nursery grounds for other species (Cathalot et al., 2015). Because of the high ecological importance of these habitats, they are described as biodiversity hotspots (Kazanidis et al., 2021). CWCs are increasingly threatened by current and imminent human activities such as bottom trawling, hydrocarbon exploitation, ocean acidification, and deep-sea mining (Buhl-Mortensen, 2017; Fosså et al., 2002; Orr et al., 2005; Reed et al., 2007). For this reason, some regions harbouring CWCs have implemented measures for their protection, such as the Habitats Areas of Particular Concern (HAPC) in Florida (Reed, 2002), or the

* Corresponding author at: Departamento de Biodiversidad y Biología Evolutiva, Museo Nacional de Ciencias Naturales (MNCN), CSIC, 28006 Madrid, Spain.
E-mail address: carlotagrsa@gmail.com (C. Gracia-Sancha).

https://doi.org/10.1016/j.ympev.2026.108697
Received 1 April 2026; Received in revised form 23 June 2026; Accepted 22 July 2026
Available online 30 July 2026

Marine Protected Areas (MPAs) established in the NE Atlantic through the EU Habitats Directive (De Santo and Jones, 2007). Importantly, during the United Nations General Assembly (UNGA) Resolution 61/105 (2006), CWCs were defined as Vulnerable Marine Ecosystems (VMEs) with the aim of protecting them from the damage caused by destructive bottom fishing methods (Grehan et al., 2004).

Conservation efforts aimed at protecting deep-sea VMEs increasingly rely on genetic connectivity studies to evaluate population structure, dispersal capacity, and species resilience within these ecosystems (Cowen et al., 2007; Wang et al., 2024). Although genetic connectivity studies in the deep sea are relatively limited, most of the studies conducted to date have focused on Crustacea, followed by Echinodermata, Mollusca and Cnidaria (see Taylor and Roterman, 2017). One of the most studied coral species to this regard is *Desmophyllum pertusum* (Linnaeus, 1758), a relatively common CWC in the North Atlantic providing important ecological functions and habitat for other species including commercial fish (Roberts et al., 2003; Arnaud-Haond et al., 2017; Costello et al., 2005; Wilson, 1979). For instance, microsatellite-based connectivity studies of *D. pertusum* across its North Atlantic distribution revealed a clear separation between eastern and western populations, likely driven by oceanographic currents limiting larval dispersal, regional differences in primary productivity, and historical vicariant processes associated with postglacial recolonization (Morrison et al., 2011). However, microsatellites and techniques providing broader genomic coverage and depth like Restriction-site Associated DNA Sequencing (RADseq) also revealed high connectivity at the regional and basin scale, likely owing to the dispersal of planktotrophic larvae with an extensive pelagic larval duration (PLD) in excess of three months along regional currents and gyres (Dahl et al., 2012; Morrison et al., 2011; Strömberg and Larsson, 2017; Weinnig et al., 2024; Capel et al., 2025). Despite high levels of genetic connectivity at the regional scale, asexual reproduction and inbreeding in this partially clonal species can result in populations with reduced levels of heterozygosity (Dahl et al., 2012; Goff-Vitry et al., 2004). Depth can also play an important role in the genetic differentiation of deep-sea bathyal fauna in general (Quattrini et al., 2015; Rex and Etter, 2010) and for *D. pertusum* in particular, in which possible vertical genetic structure has been detected in the Western North Atlantic between depths of ~ 300 m to ~ 1600 m (Morrison et al., 2011). Additionally, the use of biophysical modelling in connectivity and conservation planning provides predictive insight into larval dispersal and has revealed possible connections among *D. pertusum* populations across the Atlantic and Mediterranean (Matos et al., 2024; Guy et al., 2025).

The habitats formed by CWCs are structurally complex reefs of coral skeletons, which provide physical niches for an array of marine species and are characterized by high biomass and biodiversity (Roberts and Cairns, 2014; Rogers, 1999). The species inhabiting these CWC habitats have different reproductive systems, larval development, duration, survival and behaviour, as well as adult mobility, which directly affect dispersal capabilities (Becker et al., 2007; Montgomery et al., 2019). Therefore, a comprehensive assessment of connectivity in CWC reefs requires the inclusion of multiple co-occurring species, as connectivity patterns may vary among taxa (Jenkins and Stevens, 2018). Members of the family Eunicidae are commonly found living in association with coral reefs, with examples of species inhabiting coralline rock–coral rubbles, coralline sand, and dead corals (De León-González and Díaz, 2006; Hernández-Alcántara et al., 2019). Some eunicid species are even involved in coral reef formation, colonizing branches of living CWCs, mainly in species like *Desmophyllum pertusum* (Linnaeus, 1758) and *Madrepora oculata* Linnaeus, 1758 (Buhl-Mortensen and Mortensen, 2004; Mortensen, 2001; Roberts, 2005). Such is the case of the association between *D. pertusum* and *Eunice norvegica* (Linnaeus, 1767), described as a mutualistic symbiosis (Mueller et al., 2013). In this case, parchment-like tubes are built on the coral framework by the worm, with subsequent calcification of these structures by the coral host. The stability of the coral framework may be facilitated by connecting branches produced by the eunicid, thus generating a larger structure that possibly confers on the polyps a better positioning in the water column enhancing the feeding activity (Mueller et al., 2013; Rex and Etter, 2010). The worm also defends the coral framework from potential predators. In turn, the worms gain protection and food living inside the coral (Mueller et al., 2013).

Knowledge about the genetic connectivity in the deep-sea coral *D. pertusum* contrasts with the limited availability of connectivity studies for its symbiont *E. norvegica*. To our knowledge, there is only one brief note in a study that addressed its genetic connectivity in an analysis of individuals found in association with populations of *D. pertusum* along the NE Atlantic and the Mediterranean Sea (Boavida et al., 2019). Using an indeterminate number of RADseq-derived Single Nucleotide Polymorphisms (SNPs), limited gene flow was found between populations from the Atlantic and the Mediterranean Sea, also supported by information derived from the mitochondrial cytochrome *c* oxidase subunit I (*COI*). Boavida et al. (2019) also detected long-distance genetic connectivity between samples collected from the Bay of Biscay and Iceland. However, there is still a lack of information about the general genetic connectivity patterns of *E. norvegica* across the NE Atlantic, where both the worm and its host are widely distributed (Buhl-Mortensen et al., 2010; Mueller et al., 2013; Arnaud-Haond et al., 2017). Given the paucity of information, we investigated the genetic diversity and connectivity patterns of *E. norvegica* along the Northeast Atlantic Ocean using RADseq with the aim of informing the design of spatial conservation measures. Additionally, we examined the power of this genomic approach to separate *E. norvegica* from the closely related *Eunice philocorallia* Buchanan (1893), which is also associated with reef-forming CWCs (Buchanan, 1893). Phylogenetic analyses using mitochondrial (*COI* and *16S*) and nuclear (*18S*) genetic markers were also performed across a broader range of species, while morphological comparisons were limited to a subset of taxa. Together with ecological information, these approaches provided insights into the evolutionary relationships of eunicid species living in association with CWCs.

2. Materials and methods

2.1. Sample collection, preservation and morphological identification

Eunicidae specimens living in association predominantly with *Desmophyllum pertusum, Madrepora oculata,* and *Solenosmilia variabilis* Duncan (1873) were collected from the Northeast of the Atlantic on board *RRS James Cook* (JC136) during May and June 2016 by the remotely operated vehicle (ROV) *Isis*, as part of the NERC-funded DeepLinks project (NE/K011855/1 and NE/K013513/1), and from the Cantabrian Sea using a rock dredge on board Spanish *R/V Ángeles Alvariño*, in June 2017, as part of the SponGES0617 cruise, along a depth gradient between 200–1200 m (Fig. 1; Table 1; Supplementary Data 1). The 230 samples collected were preserved in 96% EtOH and kept at −20°C for subsequent molecular and morphological studies.

Taxonomic identification of the worms was undertaken following the original description of different Eunicidae species and additional literature (Fauchald, 1992; Gil, 2011), with a Zeiss Stemi 2000 stereoscope and an Olympus BX43 compound microscope (Olympus Corporation, Japan). For comparative purposes, in-detail morphological analyses were performed for parapodia of the segments 61, 59, and 72 only for *E. norvegica, E. philocorallia,* and *Eunice* cf. *nicidioformis* Treadwell (1906), respectively. Morphological details of *Leodice* cf. *antarctica* Baird (1869) could not be included due to the poor preservation of the specimens. Each parapodium was extracted from the right side of the worm. Pictures of the parapodia were taken under a Leica M125 stereoscope followed by more detailed pictures of the chaetae of each parapodium under an Olympus BX43 light microscope. The same parapodia of each specimen were dehydrated in an ascending ethanol series, critical-point-dried, mounted on pins and coated with gold using a sputter coater (Edwards S150B Gold Sputter Coater). Samples were

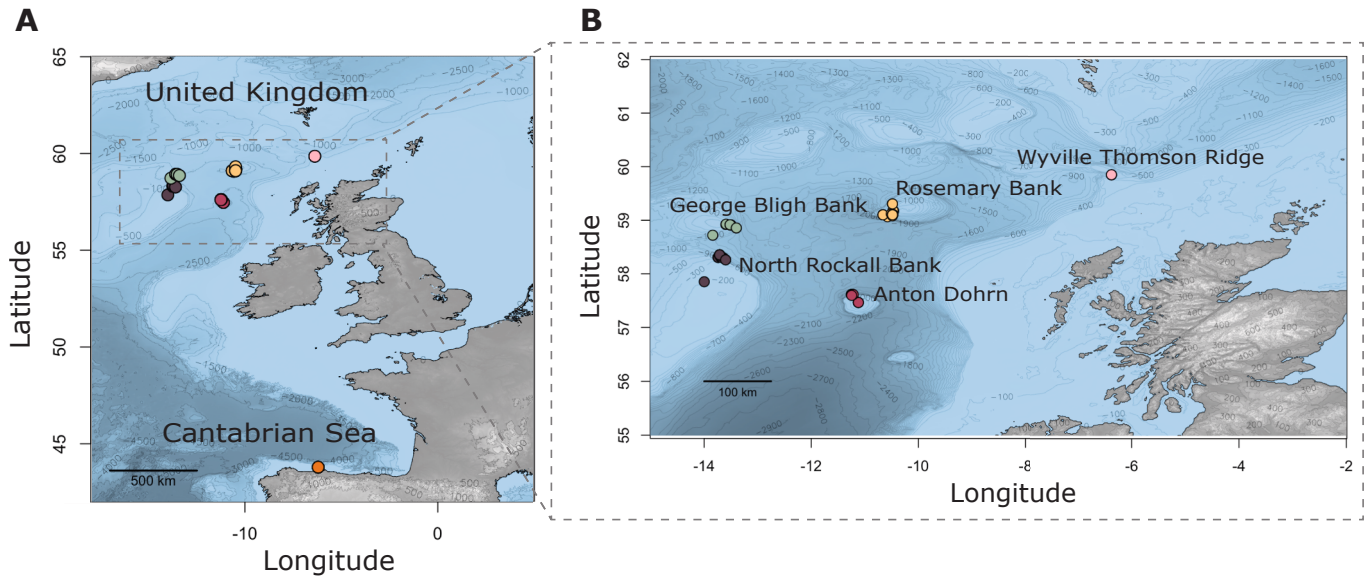

Fig. 1. (A). Map of the sampling locations where specimens of the family Eunicidae were collected; each color represents a different sampling location. (B). Detail of the sampling locations North of the United Kingdom.

later examined in a Scanning Electron Microscope (FEI INSPECT™) at the Museo Nacional de Ciencias Naturales in Madrid, Spain.

2.2. DNA extraction, amplification and sequencing

Genomic DNA was extracted from 8 to 12 midbody parapodia (depending on the size of the specimen) in order to avoid the digestive tract. This was done for a total of 230 eunicids using the DNeasy® Blood and Tissue kit (QIAGEN, Germany), following the manufacturer's protocol. DNA concentration was quantified using NanoDropTM 8000 (Thermo Fisher Scientific, USA).

Gene fragments of *COI*, *16S* rRNA (*16S*), and *18S* rRNA (*18S*) were amplified through polymerase chain reaction (PCR) (see Supplementary Data 1). *16S* amplicons were sequenced for 223 samples, while *COI* and *18S* were only amplified and sequenced for 14 specimens belonging to different phylogenetic clades. Amplified sequence data is deposited at NCBI (see Supplementary Data 1 for details). Primer pairs and PCR programs were as follows: for *COI* the primer pair consisted of ACOI-F (CWAATCAYAAAGATATTGGAAC) and COIEU-R (AATATAWACTTCWGGG TGACC) (Colgan et al., 2001; Zanol et al., 2010), and the PCR program was 94°C/5 min – (94°C/30 s – 60°C/30 s – 72°C/30 s) x 35 cycles – 72°C/5 min; *16S* was amplified using the arL (CGCCTGTTTATCAAAAACAT) and brH (CCGGTCTGAACTCAGATCA CGT) primer pair (Palumbi, 1996), and the PCR program was 95°C/5 min – (95°C/30 s, 58°C/30 s, 68°C/45 s) x 30 cycles – 68°C/10 min; and the *18S* was sequenced through three overlapping fragments, with the primer pairs 1F (TACCTGGTTGATCCTGCCAGT AG), 5R (CTTGGCAAATGCTTTCGC); 4F (CCAGCAGCCGCGCTAATTC), 7R (GCATCACAGACCTGTTATTGC); and a2.0 (GATCCTTCCGCAGGTTCACCTAC), 9R (ATGGTTGCAAAGCTGAAAC) (Giribet et al., 2002; Whiting et al., 1997), and the PCR program was 94°C/5 min – (94°C/30 s, 64°C/30 s, 72°C/1 min) x 30 cycles – 72°C/10 min.

All DNA markers were amplified in 13 μL reactions using 10 μL of VWR Red Taq DNA Polymerase 1.1x Master Mix (VWR International bvba/sprl, Belgium), 1 μL of the forward and reverse primers (totalling 2 μL), and 1 μL of DNA template. PCR products, stained with GelRed® (Biotium, USA), were visualized in a 1.5% agarose gel electrophoresis, run at 90 V for 40 min. Amplification products were purified with ExoSAP-IT (Thermo Fisher Scientific) and sequenced using the forward and reverse primers described above by MacroGen Ltd. (South Korea). Amplified sequence data is deposited at NCBI (see Supplementary Data 1 for details).

2.3. Phylogenetic and haplotype network analyses

To check the phylogenetic relationship of our specimens, consensus sequences from 14 individuals for the three different markers were generated by assembling and trimming overlapping sequence fragments using the software *Geneious* v.11.0.20.1 + 1 (Kearse et al., 2012). The resulting sequences were combined with Genbank-derived sequences from 22 different eunicid taxa, together with four outgroup polychaete species (see Supplementary Data 1). The phylogenetic analysis thus incorporated a total of 40 terminal taxa. After aligning with *MAFFT* v.7 (Katoh et al., 2019) the sequences of the three genetic markers separately, *Gblocks* v.0.91b (Castresana, 2000) was run for the non-coding genes (*16S* and *18S*) to remove ambiguous regions using the following parameters: minimum length of a block after gap cleaning: 10; no gap positions were allowed in the final alignment; all segments with contiguous non-conserved positions bigger than 8 were rejected; minimum number of sequences for a flank position: 85%. The resulting alignments were manually trimmed in *Geneious*, producing the following alignment lengths: 554 bp for *COI* containing 34 taxa, 385 bp for *16S* containing 39 taxa, and 1,131 bp for *18S* containing 39 taxa. The selection of the evolutionary models for each marker was performed using the Akaike information criterion (AIC) in *JModeltest* v.2.1.7 (Darriba et al., 2012). The best model for the three different alignments was the general time reversible (GTR) with gamma-distributed rates across sites and a proportion of invariable sites (GTR + G + I). In addition, interspecific mean pairwise genetic distances were calculated for the *16S* and *COI* alignments in R using the packages *ape* (Paradis and Schliep, 2019) and *spider* (Brown et al., 2012) (see supplementary Data 2). The concatenated alignment was run in *raxmlGUI* v.2.0 (Edler et al., 2021), which uses maximum-likelihood (ML) optimality criterion, with 10 runs and 1,000 repetitions, using GTR + I + G as evolutionary model, with partitions distinguishing between coding (*COI*) and non-coding genes (*16S* and *18S*). The *COI* gene was treated as a single coding partition without further partitioning by codon position. The resulting tree was visualized and edited in *FigTree* v.1.4.4 (Rambaut, 2018). In addition, a second tree was generated following the same procedure only with an alignment of 495 bp for *16S* sequences for our 223 eunicids together with 25 species from GenBank (248 individuals in total) (see Supplementary Data 1).

Table 1
List of the Eunicidae specimens collected in each sampling site ordered by species.

Sampling station	N	Location	Latitud	Longitud	Depth (m)	Coral Host
Eunice norvegica						
CS-DR6	5	Cantabrian Sea	43°46.565′N	6°12.266′W	1150	*Desmophyllum pertusum*
CS-DR11	1	Cantabrian Sea	43°46.3200′N	6°12.0400′W	1177	*Desmophyllum pertusum*
CS-DR12	5	Cantabrian Sea	43°46.4148′N	6°11.901′W	1151	*Desmophyllum pertusum*
CS-DR16	7	Cantabrian Sea	43°46.622′N	6°12.012′W	1018	*Desmophyllum pertusum*
AD-ROV269	1	Anton Dohrn	57°36.848′N	11°14.906′W	1219	*Solenosmilia variabilis*
AD-ROV270	11	Anton Dohrn	57°36.253′N	11°13.814′W	778–822	*Desmophyllum pertusum* *Solenosmilia variabilis* *Madrepora oculata*
AD-ROV271	11	Anton Dohrn	57°36.756′N	11°14.126′W	1046–1095	*Desmophyllum pertusum* *Solenosmilia variabilis* *Madrepora oculata*
AD-ROV272	17	Anton Dohrn	57°27.823′N	11°7.155′W	564	*Desmophyllum pertusum* *Madrepora oculata*
AD-ROV296	9	Anton Dohrn	57°36.823′N	11°13.353′W	1007–1115	*Desmophyllum pertusum* *Madrepora oculata*
NRB-ROV274	3	North Rockall Bank	57°51.084′N	13°59.885′W	191	*Desmophyllum pertusum*
NRB-ROV275	7	North Rockall Bank	58°18.343′N	13°39.365′W	852	*Desmophyllum pertusum* *Madrepora oculata*
NRB-ROV277	18	North Rockall Bank	58°18.262′N	13°44.342′W	532–557	*Desmophyllum pertusum* *Madrepora oculata*
NRB-ROV278	6	North Rockall Bank	58°18.416′N	13°41.248′W	839–864	*Desmophyllum pertusum*
NRB-ROV279	21	North Rockall Bank	58°21.11′N	13°42.673′W	931–1008	*Desmophyllum pertusum* *Solenosmilia variabilis* *Madrepora oculata*
NRB-ROV280	3	North Rockall Bank	58°15.592′N	13°35.924′W	570–590	*Desmophyllum pertusum* *Madrepora oculata*
WTR-ROV283	6	Wyville Thomson Ridge	59°51.129′N	6°22.492′W	507–519	*Desmophyllum pertusum* *Madrepora oculata*
RB-ROV286	5	Rosemary Bank	59°10.693′N	10°27.926′W	575–584	*Desmophyllum pertusum* *Madrepora oculata*
RB-ROV287	14	Rosemary Bank	59°6.005′N	10°39.309′W	902–1238	*Desmophyllum pertusum* *Madrepora oculata*
RB-ROV288	19	Rosemary Bank	59°07.200′N	10°30.432′W	819–870	*Desmophyllum pertusum* *Madrepora oculata*
RB-ROV289	1	Rosemary Bank	59°04.892′N	10°27.074′W	830	*Madrepora oculata*
RB-ROV290	3	Rosemary Bank	59°18.392′N	9°40.502′W	1053–1085	*Desmophyllum pertusum*
GBB-ROV281	2	George Bligh Bank	58°43.131′N	13°50.36′W	767–828	*Desmophyllum pertusum* *Madrepora oculata*
GBB-ROV291	3	George Bligh Bank	58°55.454′N	13°35.642′W	548–564	*Desmophyllum pertusum*
GBB-ROV293	7	George Bligh Bank	58°54.859′N	13°30.593′W	783–845	*Desmophyllum pertusum* *Madrepora oculata*
GBB-ROV295	3	George Bligh Bank	58°51.321′N	13°23.959′W	1050–1052	*Madrepora oculata*
Eunice philocorallia						
AD-ROV271	2	Anton Dohrn	57°36.985′N	11°14.292′W	1258–1260	*Solenosmilia variabilis*
AD-ROV296	2	Anton Dohrn	57°36.884′N	11°14.911′W	1202–1280	*Solenosmilia variabilis*
Eunice* cf. *nicidioformis						
CS-DR5	1	Cantabrian Sea	43°46.631′N	6°12.204′W	1036	*Desmophyllum pertusum*
CS-DR6	5	Cantabrian Sea	43°46.565′N	6°12.266′W	1150	*Desmophyllum pertusum*
CS-DR11	2	Cantabrian Sea	43°46.3200′N	6°12.0400′W	1177	*Desmophyllum pertusum*
CS-DR12	8	Cantabrian Sea	43°46.4148′N	6°11.901′W	1151	*Desmophyllum pertusum*
CS-DR16	20	Cantabrian Sea	43°46.622′N	6°12.012′W	1018	*Desmophyllum pertusum*
Leodice* cf. *antarctica						
CS-DR11	1	Cantabrian Sea	43°46.3200′N	6°12.0400′W	1177	*Desmophyllum pertusum*
CS-DR12	1	Cantabrian Sea	43°46.4148′N	6°11.901′W	1151	*Desmophyllum pertusum*
Total	**230**					

For the haplotype network analyses, the *16S* sequence alignment was manually trimmed in *Geneious* for 181 *E. norvegica* specimens (553 bp) and 36 *E.* cf. *nicidioformis* individuals (547 bp). The remaining species were excluded from these analyses due to insufficient sample sizes (see Supplementary Data 1). The software *PopART* v.1.7.2 (Leigh and Bryant, 2015) was used for building haplotype networks for each species separately, using the TCS algorithm (Clement et al., 2000). *Eunice norvegica* specimens were grouped by sampling station and by depth ranges (<530 m, 530–780 m and > 780 m), while *E.* cf. *nicidioformis* was grouped by sampling station only. Polymorphic sites and levels of DNA polymorphism were calculated for the *16S* in *E. norvegica* and *E.* cf. *nicidioformis* for the different sampling stations using the *DNASP* v.6.12.03 (Rozas et al., 2017) and included number of haplotypes (*H*), private haplotypes (*Hp*), haplotype diversity (*Hd*), polymorphic sites (*Np*), and nucleotide diversity (π) (Table 2). To infer historical demographic processes, Tajima's *D* neutrality test (Tajima, 1989) was calculated for the different sampling stations, in which more than three individuals were available, for both species in RStudio v.4.4.1 (R Core Team, 2024) using the *ape* package (Paradis and Schliep, 2019) and the *pegas* package (Paradis, 2010) (Table 2).

2.4. Radseq library preparation and sequencing

RADseq libraries were constructed for a total of 119 individuals, including 115 *E. norvegica* specimens from the Cantabrian Sea and the United Kingdom and four specimens of *E. philocorallia* from the United Kingdom. Genomic (g) DNA was quantified with the Qubit dsDNA BR Assay Kit (Thermo Fisher), and the presence of high molecular weight

Table 2
Haplotype diversity metrics for the *16S* in *Eunice norvegica* and *Eunice* cf. *nicidioformis*. *N* number of individuals; *H* number of haplotypes; *Hp* private haplotypes; *Np* number of polymorphic sites; *Hd* haplotype diversity; π nucleotide diversity. Significant values ($p > 0.05$) of Tajima's *D* in bold.

	N	H	Hp	Np	Hd	π	Tajima's *D*
Eunice norvegica							
Anton Dohrn	48	8	7	11	0.598 ± 0.080	0.002 ± 0.000	**−1.840**
Cantabrian Sea	16	2	0	1	0.400 ± 0.012	0.001 ± 0.000	**−2.544**
George Bligh Bank	15	3	3	4	0.448 ± 0.134	0.002 ± 0.001	−1.071
North Rockall Bank	57	4	2	4	0.634 ± 0.032	0.002 ± 0.000	−0.176
Rosemary Bank	39	4	3	4	0.279 ± 0.089	0.001 ± 0.000	**−1.824**
Wyville Thomson Ridge	6	2	1	1	0.333 ± 0.215	0.001 ± 0.000	−0.933
Total	181	9	–	7	0.524 ± 0.039	0.002 ± 0.000	–
Eunice* cf. *nicidioformis							
CS-DR5	1	–	–	0	–	–	–
CS-DR6	5	2	1	1	0.400 ± 0.237	0.001 ± 0.001	**−5.311**
CS-DR11	2	2	0	0	0.000 ± 0.000	0.000 ± 0.000	–
CS-DR12	8	1	0	0	0.000 ± 0.000	0.000 ± 0.000	**−2.862**
CS-DR16	20	2	1	1	0.100 ± 0.088	0.000 ± 0.000	**−3.089**
Total	36	2	1	1	0.056 ± 0.052	0.000 ± 0.000	–

DNA was confirmed with 0.8% agarose gel electrophoresis. The gDNA was normalized to 20 ng/μl in 50 μl volumes and sent to Floragenex (Beaverton, OR). DNA libraries were constructed using the 6-cutter *PstI* enzyme, followed by sequencing 100 bp single-end reads across four lanes of an Illumina HiSeq2500 (University of Oregon's Genomics and Cell Characterization Core Facility lab). The Illumina short reads (sequenced RAD sites) were deposited at the NCBI Short Read Archive (SUB16085733).

2.5. Radseq locus assembly and filtering

Quality filtering and locus assembly was conducted with the *Stacks* pipeline v.2.55 (Catchen et al., 2013). The filtering and locus assembly was first conducted for the 119 individuals including specimens from *E. norvegica* and *E. philocorallia* for species delimitation analysis and then removing the four individuals of *E. philocorallia* for population genomics analysis within *E. norvegica*. Using *process_radtags,* raw sequenced reads were de-multiplexed and quality-trimmed to remove reads of low quality, reads with uncalled bases and reads without complete barcode or restriction cut site. After demultiplexing and filtering, a total of 611,211,705 reads were retained from the total 697,954,163 raw reads, representing 87.6% of the initial dataset. Read losses were primarily due to unrecognized barcodes (8.55%), low-quality reads (0.56%), and the absence of the expected RAD cut site (3.30%).

We conducted optimization tests for the *Stacks* parameters following the same approach described in Taboada et al. (2023), and based on suggestions by Jeffries et al. (2016) and Paris et al. (2017). This parameter optimization resulted in selecting the parameters *m* (minimum stack depth) = 3, *M* (maximum distance within individuals) = 2, and n (number of mismatches between catalog stacks) = 1. The output of the *Stacks denovo_map.pl* module recovered a mean locus coverage of 78.1% ± 16.1%, ranging from 33% to 124.8%. The *Stacks populations* module was run to filter data with r (minimum per population proportion of individuals per population with a locus for it to be included) = 0.6 for the species delimitation analyses and r = 0.7 for the population genomics of *E. norvegica*. Only one putative SNP (*–write_single_SNP*) was used per locus to minimize the influence of linkage disequilibrium (Catchen et al., 2013). SNPs with a minor allele frequency (MAF) < 0.05 (*–min_maf* < 0.05) within two populations were discarded in order to diminish errors in the estimation of SNPs showing signatures of selection (Benestan et al., 2015; Roesti et al., 2012; Xu et al., 2017). SNPs showing an excess of heterozygosity (*Ho* > 0.5) were removed as well (Benestan et al., 2015; Hohenlohe et al., 2011). Finally, markers departing Hardy-Weinberg equilibrium (*p*-value = 0.05) were removed when present in at least two different locations for the population genomics dataset of *E. norvegica*. The dataset used for species delimitation retained 1,886 SNPs, as the removal of SNPs under selection, applied in the population genomics dataset, was not performed.

2.6. Detection of SNPs under selection

To assess population connectivity within *E. norvegica,* SNPs potentially under selection were removed using two different selection detection approaches to ensure that analyses reflect neutral demographic processes (Beaumont and Nichols, 1996; Luikart et al., 2003). *ARLEQUIN* v.3.5.2 (Excoffier and Lischer, 2010) creates coalescent simulations to compare observed data with theoretical expectations under a given model (Schneider et al., 2000). The 'Allowed missing level per site' was set to 0.05, and the 'Non-hierarchical Island model' was employed. 100,000 simulations and 100 demes per group were performed; *p*-values obtained were corrected using the *p.adjust* function in R with the *fdr* method, corresponding to the 'BH' procedure (Benjamini & Hochberg, 1995). In contrast, *BAYESCAN* v.2.1 (Foll and Gaggiotti, 2008) is based on a logistic regression model to decompose locus-population *Fst* coefficients into a population-specific (beta) and a locus-specific (alpha) component for outlier detection. SNPs under selection were selected when having a *q-value* > 0.05, which is the FDR analogue of the *p*-value. Both *ARLEQUIN* or *BAYESCAN* identify SNPs with high *Fst* values to be potentially under divergent selection, while those being close to zero, are candidates for balancing selection. 1,067 neutral SNPs were finally retained after the removal of two SNPs under selection.

2.7. Species delimitation and population genomics analyses using SNPs

We assessed population structure using three different methods: *STRUCTURE* v.2.3 (Pritchard et al., 2000), the discriminant analysis of principal components (*DAPC*) as implemented in the *adegenet* R package (Jombart et al., 2010), and *fineRADstructure* (Malinsky et al., 2018). The *STRUCTURE* software implements a Bayesian clustering method to determine the most likely number of populations (*k*) (Pritchard et al., 2000) and was used to establish the genetic divergence between the two sister species (*E. norvegica* and *E. philocorallia*) using 119 specimens, and to define the population structure among locations of *E. norvegica*. The software was run with 200,000 Markov chain Monte Carlo (MCMC) iterations using the admixture model, with a burn-in of 100,000 iterations, setting a putative *k* from 1 to 6, with 15 replicates for each run. *STRUCTURE HARVESTER* (Earl and vonHoldt, 2012) and *CLUMPP* v.1.1.2 (Jakobsson and Rosenberg, 2007) were used to determine the most likely number of clusters and to average each individual's membership coefficient across the *k* value replicates, respectively.

DAPC analyses were performed on both the *E. norvegica* dataset and the combined *E. norvegica* and *E. philocorallia* datasets and were assessed by the function *snapclust* using the genetic clustering mode *snapclust choose k*. This was done using the Akaike Information Criterion (AIC) function with the *k*-means algorithm (*pop.ini* = *"kmeans"*), allowing a maximum *k* (*number of clusters*) of 16 (max = *16*), and a maximum number of iterations of 100 (max.*iter* = *100*). K-means was run

sequentially with increasing values of *k* to assess the optimal number of clusters (the lowest AIC value). The *DAPC* analyses involved grouping samples based on their geographical location. As no structure was found for the *E. norvegica* dataset, we considered each sample location as a separate population. The optimal number of principal component axes were selected using cross-validation with the *xvalDapc* function from the *adegenet* R package with 1,000 replicates (*n.rep = 1000*). The *DAPC* function *scatter plot* was used to produce scatterplots of PCs with eigen values as inset and *assignplot* function employed to plot the probabilities of assignment of the different individuals to the different clusters.

fineRADstructure v.0.3.2 was used to both support the species delimitation of *E. norvegica* and *E. philocorallia* and also to investigate the shared coancestry within *E. norvegica* and to provide further support to the previous *STRUCTURE* and *DAPC* analyses. The SNP dataset used in *fineRADstructure* was obtained after running *populations* on the combined dataset of both species (i.e. 1,886 neutral SNPs) deselecting the *–write_single_SNP* option, which allowed for the inclusion of linked SNPs in the different RAD-tags, resulting in a total of 19,834 SNPs. *fineRADstructure* was run with the default values: −x (number of MCMC burn-in iterations) = 100,000, −y (number of sampling iterations) = 100,000, −z (thinning interval) = 1,000 to assign individuals to populations, and −x 10,000 for the tree building. Output figures were generated using the Finestructure R Library and the fineRADstructurePlot.R script, both provided in the *fineRADstructure* package.

Genetic diversity and demographic statistics were calculated only for the *E. norvegica* dataset for a total of six different locations (Table 3). Expected (*He*) and observed (*Ho*) heterozygosity, and inbreeding coefficients (F_{ST}) were calculated per location and globally using *Stacks*.

2.8. Migration and population assignment

Gene flow patterns were investigated for all the individuals of *E. norvegica* used in the RADseq analyses, grouped by location. This was done using the *divMigrate* function of the *diveRsity* R package (Keenan et al., 2013), under the *Nm* method (Alcala et al., 2014) with no bootstrap support. In addition, we performed a population assignment analysis in order to predict the origin of the individuals. Likelihood ratio thresholds were calculated based on the Monte Carlo Likelihood ratio test with zero frequencies replaced by 0.005, an α of 0.002, and 5,000 replicated datasets using *Genodive* v.3.02 (Meirmans and Van Tienderen, 2004). Schematic pathways for Eastern North Atlantic Central Water (ENACW) and Mediterranean Water (MW) were adapted following circulation models (Jia et al., 2007; Liu and Tanhua, 2021). Sampling stations were plotted using their geographic coordinates.

Table 3
Population genetic statistics based on SNPs obtained from RADseq for *Eunice norvegica.* Samples grouped by location. *N* number of samples, *He* expected heterozygosity, *Ho* observed heterozygosity.

Sampling location	N	Private alleles	Private alleles/N	*He*	*Ho*
Cantabrian Sea	5	29	0.3	0.049 ± 0.016	0.036 ± 0.013
Anton Dohrn	37	195	1.7	0.057 ± 0.011	0.037 ± 0.006
North Rockall bank	31	187	1.6	0.064 ± 0.013	0.041 ± 0.007
George Bligh Bank	12	81	0.7	0.059 ± 0.014	0.038 ± 0.009
Rosemary Bank	28	168	1.5	0.057 ± 0.012	0.039 ± 0.007
Wyville Thomson Ridge	2	15	0.1	0.032 ± 0.013	0.036 ± 0.024
Total	115			0.062 ± 0.011	0.039 ± 0.001

3. Results

3.1. Phylogenetic and morphological analyses of Eunicidae

The 230 eunicids collected belonged to four different species from two genera. The diversity of eunicids was mostly evident in the Cantabrian location, where we detected three different taxa: *E. norvegica*, *E.* cf. *nicidioformis,* and *L.* cf. *antarctica*. Near the United Kingdom only two different species were identified: *E. norvegica* and *E. philocorallia* (Table 1).

Our Maximum-likelihood phylogenetic tree built with a concatenated alignment of *16S*, *COI,* and *18S* recovered Eunicidae as monophyletic although with no bootstrap support (Fig. 2). Representatives of the family Eunicidae were recovered in two well-supported clades including different genera. The first clade included representatives of the genus *Nicidion* Kinberg (1865), recovered as monophyletic, being sister with another *Eunice* clade, comprising *Eunice filamentosa* Grube (1856), *E. philocorallia,* and *E. norvegica.* All our *E. norvegica* specimens clustered together in a well-supported clade including the only *E. norvegica* specimen from GenBank included in the analysis, originally collected from Norway. The *E. norvegica* clade was sister to our four specimens identified morphologically as *E. philocorallia*, with a good support value; a topology also recovered with the *16S* phylogenetic tree (see Supplementary Data 3). The other well-supported clade identified in Eunicidae included samples from the genus *Leodice* Lamarck (1818) and *Eunice*, with *Eunice* being retrieved as polyphyletic. The specimens sequenced in our study clustered in three different clades: *Leodice* cf. *antarctica* clustered together with *Leodice antarctica* collected from Antarctica and formed a well-supported clade with *Leodice americana* (Hartman, 1944); specimens identified as *E.* cf. *nicidioformis* appeared in a fully-supported clade as sister to *Leodice torquata* (Quatrefages, 1866), *Leodice thomasiana* (Augener, 1922), and *Leodice marcusi* (Zanol et al., 2000) (Fig. 2).

We studied the morphological external features of specimens of *E. norvegica*, *E. philocorallia,* and *E.* cf. *nicidioformis*, which align with previous reported morphological data described by Fauchald in 1992. Due to the poor preservation state of the *L.* cf. *antarctica* specimens from the Cantabrian Sea, morphological characterization was not possible. Consequently, specimen identification relied exclusively on molecular data, supported by their phylogenetic placement (Fig. 2) and the low genetic divergence from *L. antarctica* in mitochondrial markers (0.4% for *16S* and 1.5% for *COI*; see Supplementary Data 2). The three *Eunice* species presented biramous parapodia with developed notopodia and neuropodia with differences in the shape and structure of lobes and cirri (Fig. 3A-C). Generally, aciculae were emerging at the top or at the middle of the lobe. Neurochaetae morphotypes characteristic of *Eunice* specimens were observed for the three species including, dark brown aciculae (Fig. 3A-C), dark brown and bidentate subacicular hooks (Fig. 3A-C), bidentate compound falcigers (Fig. 3D-I), heterodont pectinate chaetae (Fig. 3J-L) and distally serrated limbate chaetae (Fig. 3M-O).

3.2. Population genetic structure using 16S

The *16S* haplotype network for *E. norvegica* was generated with 553 bp sequence alignment with 181 individuals across six different locations (Fig. 4A) and three different depth ranges (Fig. 4B). A total of nine haplotypes were identified and defined by seven polymorphic sites (Fig. 4A-B, Table 2). The number of haplotypes differed among locations, ranging between two at the Wyville Thomson Ridge and 11 at the Anton Dohrn seamount. Among these haplotypes, H1 was the predominant (120 individuals), followed by H2 (26 individuals), and H3 (24 individuals). No particular structure or clustering was observed between the individuals grouped by location or by depth as haplotypes were shared between the different locations and across all depth ranges (Fig. 4A, 4B). The haplotype network was star-like, with most

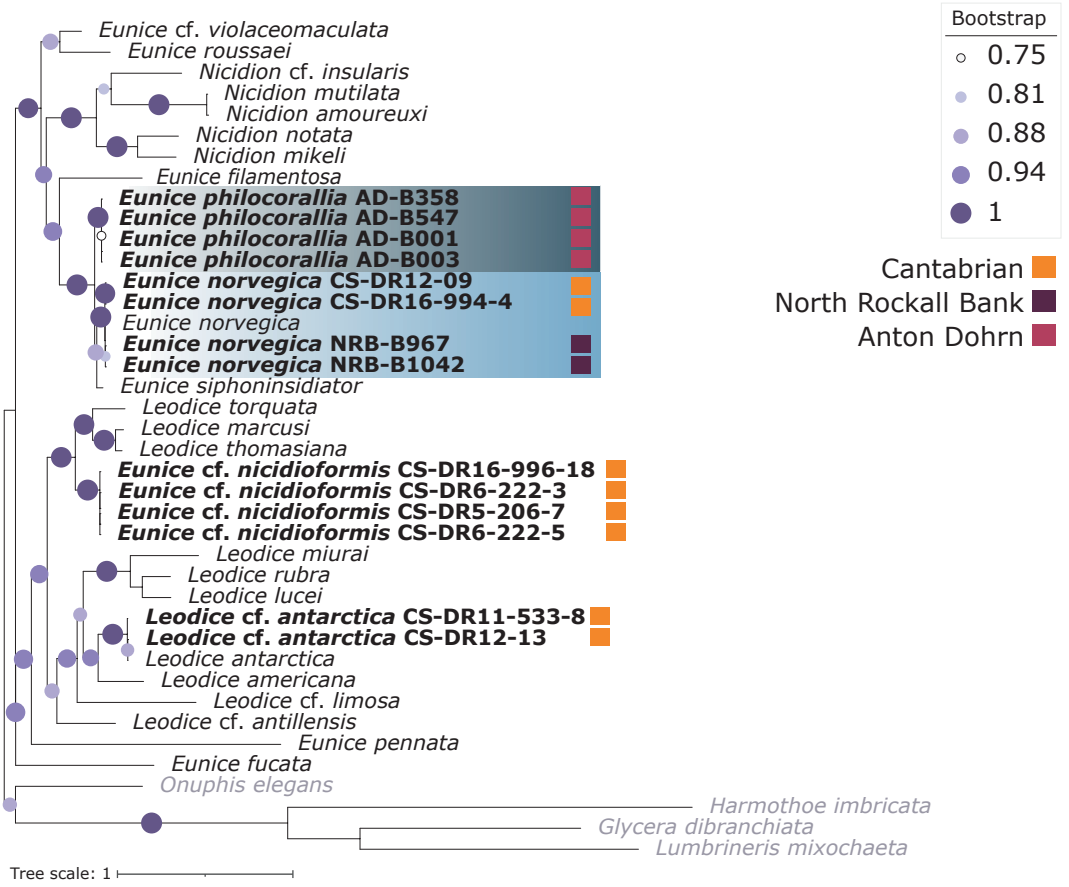

Fig. 2. Phylogenetic tree based on a concatenated analysis of *COI*, *16S* and *18S* using Maximum likelihood (ML). Specimens sequenced in the study are in bold. Only bootstrap values > 0.75 are reported with circles, where bootstrap support increases proportionally with the size of the circle and the darkness of the purple color. Colored squares show the sampling locations. (For interpretation of the references to colour in this figure legend, the reader is referred to the web version of this article.)

haplotypes deviating by only one or two basepairs from the common haplotypes (Fig. 4A).

The genetic diversity of *E. norvegica* was moderate, with an overall haplotype diversity (*Hd*) of 0.524 (± 0.039), with the highest value for North Rockall Bank (0.634 ± 0.032) and the lowest for Rosemary Bank (0.279 ± 0.089). Nucleotide diversity (π) was 0.002 (± 0.000) for the whole dataset and ranged between $\pi = 0.002$ (± 0.001) for George Bligh Bank to $\pi = 0.001$ (± 0.000) for the Cantabrian Sea, Rosemary Bank and Wyville Thomson Ridge (Table 2). Significant negative Tajima's *D* values were detected in the Anton Dohrn (−1.840), Cantabrian Sea (−2.544), and Rosemary Bank (−1.824) populations.

Eunice cf. *nicidioformis* was only found in the Cantabrian Sea and no genetic structure was observed among sampling stations. Only two haplotypes were found within the 547 bp *16S* alignment, with the most common (H1) comprising 97% of the samples and being present in all the sampling locations; these two haplotypes were only separated by a single mutational step (Fig. 4C). Haplotype diversity (*Hd*) for the whole dataset was low (0.056 ± 0.052), with the highest value for CS-DR6 (0.400 ± 0.237). Nucleotide diversity (π) ranged between $\pi = 0.001$ ± 0.001 for DR6 to $\pi = 0.000$ ± 0.000 for DR11, DR12 and DR16 (Table 2). Significant negative Tajima's *D* values were found in sites CS-DR6 (−5.311), CS-DR12 (−2.862), and CS-DR16 (−3.089).

3.3. Species delimitation using SNPs

The two sister species *E. norvegica* and *E. philocorallia* occurring in sympatry North of the United Kingdom were analysed using the RADseq-derived SNPs in order to evaluate their genetic similarity. The optimal number of genetic clusters detected by *STRUCTURE* was four ($k = 4$) (see Supplementary Data 4), with *E. philocorallia* being fully assigned to the dark blue genetic cluster, thus clearly separating this species from *E. norvegica* (Fig. 5A). *Eunice norvegica* specimens were predominantly assigned to the blue genetic cluster with a consistent, but minor contribution from the light blue cluster and a variable and sometimes high (>50%) contribution from the purple cluster (Fig. 5A). Fifteen individuals showing high levels of admixture with the purple cluster included samples from North Rockall Bank (NRB-B1042, NRB-B1043, NRB-B1049, NRB-B1050, NRB-B1051, NRB-B1052, NRB-B1053, NRB-B994, NRB-B967, NRB-B965, NRB-B1264, NRB-B1250) at 534–570 m, George Bligh Bank (GBB-B2059) at 781 m, and Anton Dohrn (AD-B677, AD-B700) at 562–564 m. Similar results were obtained in the *DAPC* analysis with samples being grouped in three different clusters (BIC = 1; AIC = 3) (Supplementary Data 4) (Fig. 5B). These clusters clearly separated specimens belonging to both species and also showed some degree of differentiation between 14 samples within *E. norvegica,* represented in purple, which correspond to the same individuals that showed a high proportion of assignment to the purple cluster in the *STRUCTURE* analysis except for the sample AD-B677, that was assigned to the blue cluster in the *DAPC* analysis and showed a high proportion of assignment to the purple cluster < 25% in the *STRUCTURE* plot (Fig. 5A-B).

The *fineRADstructure* analysis represented in the coancestry matrix depicts a clear differentiation between the two species, with *E. philocorallia* samples appearing as the most divergent from the other specimens in this study (dark blue cluster) (see Supplementary Data 5). All *E. norvegica* samples grouped together although 3 subclusters could

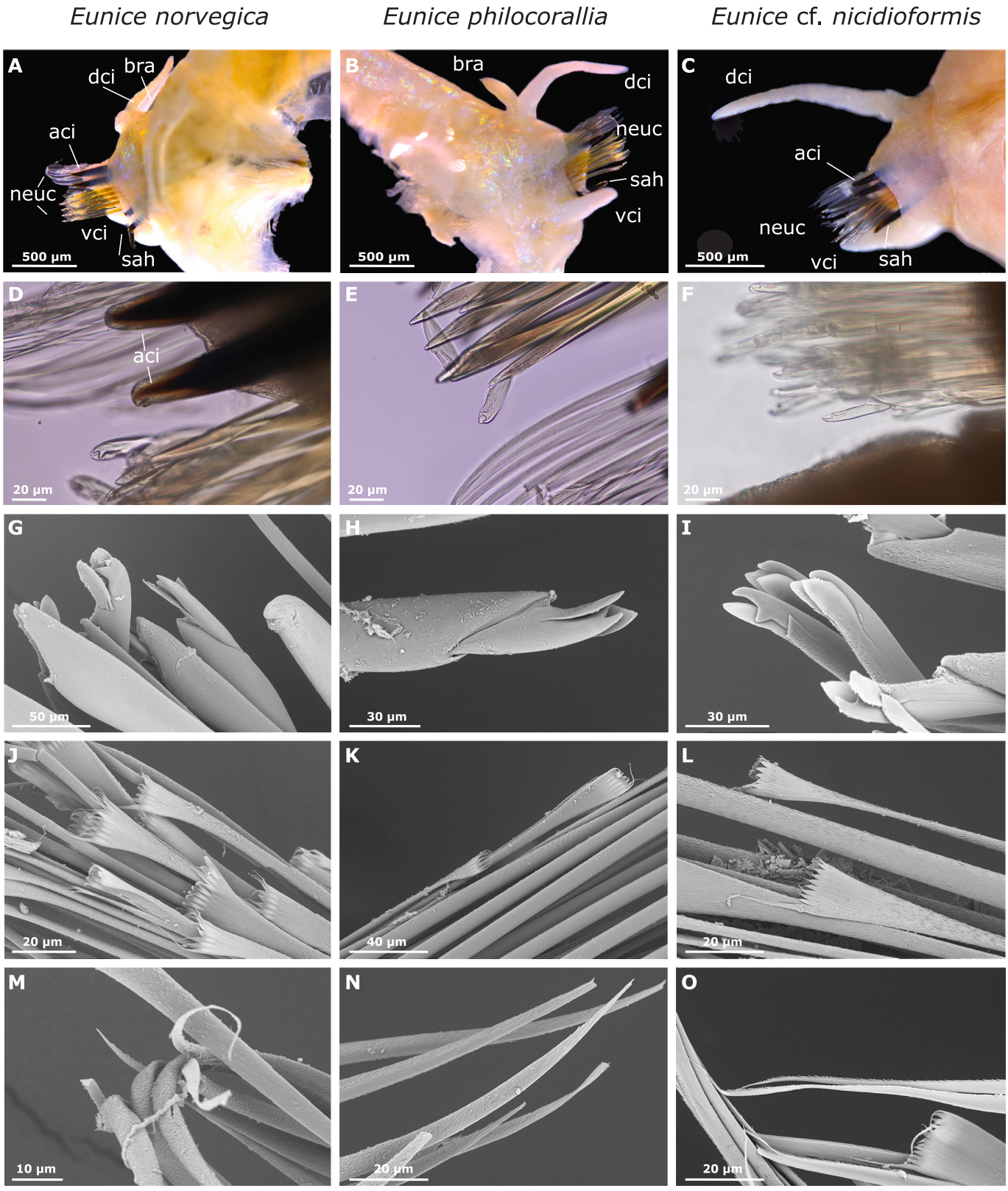

Fig. 3. Parapodia and chaetae of *Eunice norvegica* (A, D, G, J, M), *Eunice philocorallia* (B, E, H, K, N) and *Eunice* cf. *nicidioformis* (C, F, I, L, O). **A-C**. Parapodia under stereomicroscope. *Eunice norvegica* parapodium 61, anterior view (A); *E. philocorallia* parapodium 59 posterior view (B); *E.* cf. *nicidioformis* parapodium 72, anterior view (C). **D-F**. Light microscopy images of the compound falcigers. **G-I**. SEM microscopy images of the compound falcigers. **J-L**. SEM microscopy images of pectinate chaetae. **M**—**O**. SEM microscopy images of limbate chaetae. Abbreviations: *aci* aciculae; *bra* branchia; *dci* dorsal cirrus; *neuc* neurochaetae; *sah*: subacicular hook; *vci* ventral cirrus.

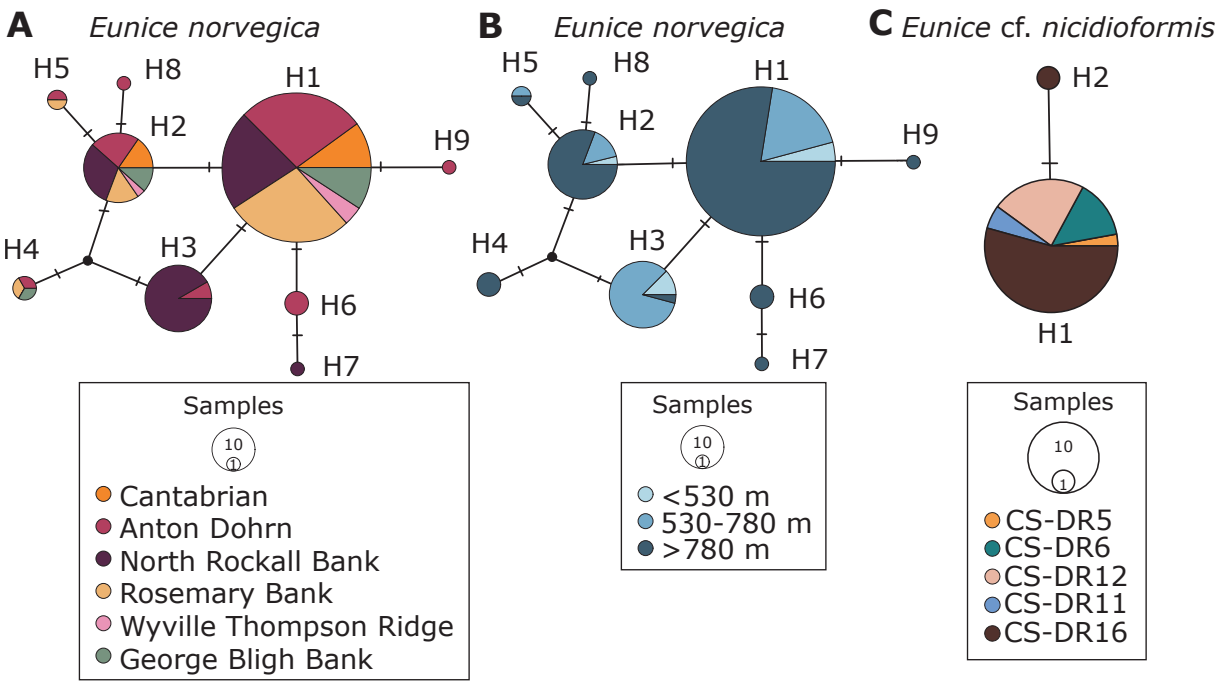

Fig. 4. Haplotype network based on *16S* for *Eunice norvegica* (A-B) and *Eunice* cf. *nicidioformis* (C). Circles are proportional to the number of individuals for each haplotype. Cross lines symbolize the mutational steps and missing inferred haplotypes are in black. (A). *Eunice norvegica* haplotype network color coded by sampling location (N = 181). (B). *Eunice norvegica* haplotype network color coded by depth ranges (N = 181). (C). *Eunice* cf. *nicidioformis* haplotype network color coded by sampling stations within the Cantabrian Sea (N = 36).

be differentiated. Subcluster 1 grouped the 15 samples that appeared differentiated in the *STRUCTURE* plot; Subcluster 3 was formed by two samples from Anton Dohrn (AD-B2264, AD-B2265) at 1024 m; and Subcluster 2 comprised the rest of *E. norvegica* samples with two samples from Anton Dohrn showing a higher degree of coancestry with respect to the other subclusters (AD-B611, AD-B619) at 564 m.

3.4. Population genomic structure and connectivity using RADseq-derived SNPs

Statistics for the population genetics of each of the six locations where *E. norvegica* was collected are detailed in Table 3. The number of private alleles was quite uneven, being the highest for Anton Dohrn (195) and the lowest for Wyville Thomson Ridge (15). The number of private alleles per individual was again the highest for Anton Dohrn (1.7) and the lowest for Wyville Thomson Ridge (0.1).

Overall, the genetic diversity, measured with the expected heterozygosity (*He*), was relatively low (0.062 ± 0.011) for the whole dataset, with similar values for the different locations, with the highest values for North Rockall Bank (0.064 ± 0.013) and the lowest for the Cantabrian Sea (0.049 ± 0.016), although here we did not take into consideration Wyville Thomson Ridge (0.032 ± 0.013), with only two samples. Observed heterozygosity (*Ho*) presented similar values to those obtained for the *He*, with an overall value of 0.039 ± 0.001, and with values ranging 0.041 ± 0.007 for North Rockall Bank and 0.036 ± 0.013 for the Cantabrian Sea (Table 3).

The optimal number of clusters detected by *STRUCTURE* was three ($k = 3$) (see Supplementary Data 6), with no clear differentiation between samples except for the same 15 individuals that appeared differentiated in the species delimitation analyses from North Rockall Bank (NRB-B1042, NRB-B1043, NRB-B1049, NRB-B1050, NRB-B1051, NRB-B1052, NRB-B1053, NRB-B994, NRB-B967, NRB-B965, NRB-B1264, NRB-B1250), George Bligh Bank (GBB-B2059), and Anton Dohrn (AD-B677, AD-B700). All these individuals showed a variable degree of assignment to the purple cluster (<50%) into the predominant blue cluster (Fig. 6A). *DAPC* analysis found no genetic differentiation among samples (BIC = 1; AIC = 1) (Supplementary Data 6). Our *DAPC* analysis grouping samples per location again showed no clear differentiation between locations with the exception of the 15 individuals mentioned above that showed a subtle genetic differentiation with respect to the rest of samples (Fig. 6B).

Pairwise *Fst* comparisons for the six locations of *E. norvegica* were relatively low, ranging from 0.004 for the comparison between Anton Dohrn with Rosemary Bank, to 0.100 for the comparison observed between North Rockall Bank and Wyville Thomson Ridge (Table 4).

Migration analyses on the *E. norvegica* dataset showed bidirectional migration between the locations North of the United Kingdom, except for Wyville Thomson Ridge (Fig. 7A). The higher migration rates appeared from Anton Dohrn towards Rosemary Bank (1) and North Rockall Bank (0.95), while the lower signs of migration were observed from the Cantabrian Sea to the rest of locations (Fig. 7A). The population assignment analysis revealed that individuals from North Rockall Bank, Anton Dohrn, and Rosemary Bank are the major contributors for the remaining locations (Fig. 7B). A minor genetic contribution from George Bligh Bank was only observed in the Rosemary Bank location. Notably, individuals from Wyville Thomson Ridge appeared to originate exclusively from Rosemary Bank, while samples from the Cantabrian Sea were assigned to either Anton Dohrn or North Rockall Bank (Fig. 7B). These migration dynamics are affected by the regional current systems, predominantly mediated by the northward flow of the Mediterranean Water (MW) and the North Atlantic Central Water (ENACW) (Fig. 7C).

4. Discussion

4.1. Eunicid diversity and distribution

In our study we documented the diversity of deep-sea eunicids living in association with CWCs across different sampling locations in the NE Atlantic, finding four distinct species belonging to two different genera (Table 1). The distribution of *E. norvegica* has been previously reported, with its occurrence spanning the whole Atlantic Ocean (type locality in the Norwegian Sea (Linnaeus, 1767) but also being reported from South

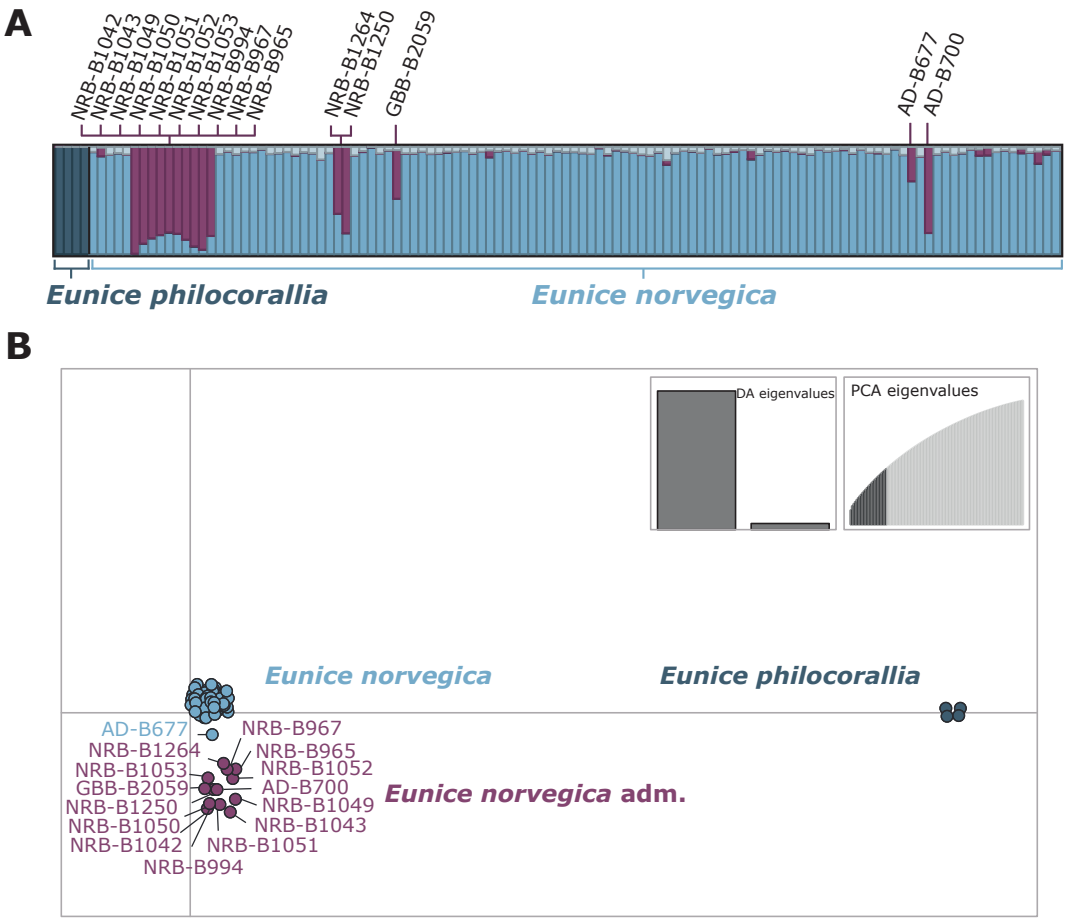

Fig. 5. (A). Individual genotype assignment based on SNPs obtained from RADseq of *Eunice norvegica* and *Eunice philocorallia* to clusters (*k*) as inferred by *STRUCTURE* for the whole dataset with $k = 4$. Each vertical bar represents an individual whereas each color a different genetic cluster (*k*). Labels in some individuals represent the ones with a relatively high percentage of admixture of the purple cluster (B). *DAPC* analysis of the whole dataset. Each point represents one individual. *Eunice philocorallia* are represented in dark blue, while we differentiate two clusters of samples for *E. norvegica*: one in blue and another in purple (*Eunice norvegica* adm.). (For interpretation of the references to colour in this figure legend, the reader is referred to the web version of this article.)

Africa and the Mediterranean Sea deeper than 200 m depth (Carlier et al., 2009; Gravina et al., 2021; Sağlam and Sarieyyüpoğlu, 2008; Winsnes, 1989; Fauchald et al., 2009; Leland, 1998). For *E. philocorallia*, to our knowledge only a few studies have documented its distribution, only noting its presence from the coasts of Ireland up to Norway at depths around 300 m (Haddon, 1895; Hickson, 1907; M'Intosh, 1903). Thus, we documented here the deepest records for *E. philocorallia,* extending its bathymetric range to 1,280 m. In our study we also reported the presence of *E.* cf. *nicidioformis* and *L.* cf. *antarctica* in the Cantabrian Sea, both of them recorded, to our knowledge, for the first time in this location, at depths deeper than 1,000 m. *Eunice* cf. *nicidioformis* was originally described from the Pacific Ocean (Treadwell, 1906), so the assumption that these individuals belong to this species is based, on the one hand, on later records from the Azores archipelago (Central Atlantic Ocean) at depths of around 400 m (Gillet and Dauvin, 2003), and on the similarity of their morphological characters. However, this species has only been reported from depths of less than 500 m, whereas our individuals were collected at around 1000 m depth. Therefore, this identification should be treated with caution. Interestingly, although our *Leodice* cf. *antarctica* specimens clustered together with *Leodice antarctica* collected from Antarctic waters in a fully supported clade in our phylogenetic analysis, their assignment to this species remains uncertain considering that *L. antarctica* appears to have a documented distribution in the Southern Ocean, the SubAntarctic Kerguelen Islands, and Indonesia (Baird, 1869; Zanol et al., 2010; Liline et al., 2017). However, wide distributions are not uncommon in the deep sea, with several marine invertebrates, particularly annelids, occurring across distant basins, including shared species between the Antarctic and other remote deep-sea areas (Eilertsen et al., 2018). Nevertheless, since our *Leodice* cf. *antarctica* individuals could not be morphologically studied, the identification to species level should be considered tentative.

All of the eunicids sampled in this study were predominantly found in close association with the branches of scleractinian corals from deep-water coral reefs (see Supplementary Data 1). The symbioses of *Eunice* worms with scleractinian corals has been studied before, particularly regarding *Desmophyllum pertusum* and *E. norvegica*, where the possible mutual benefits of the interaction have been well explored (De Clippele et al., 2015; Mortensen, 2001; Mueller et al., 2013). The three different coral species associated with the worms included in the present study were *D. pertusum*, *Solenosmilia variabilis,* and *Madrepora oculata*. Specimens of *E. norvegica* were found in all three species (Table 1), consistently with previous reports (Mortensen, 2001; Roberts, 2005; Almón et al., 2014). Notably, *E.* cf. *nicidioformis* and *Leodice* cf. *antarctica,* two eunicids never previously reported living in association with any coral, were also recovered in close association with *D. pertusum*. In this study we also found *E. philocorallia* living in association with *S. variabilis*, but not *D. pertusum* – and only at depths greater than 1000 m, whereas in the original description of the worm it was reported inside the branches of *D. pertusum* collected from depths of around 200 fathoms (~366 m) 50 miles off the Southwestern coast of Ireland (Buchanan, 1893). The discrepancy between the depth and species association reported for

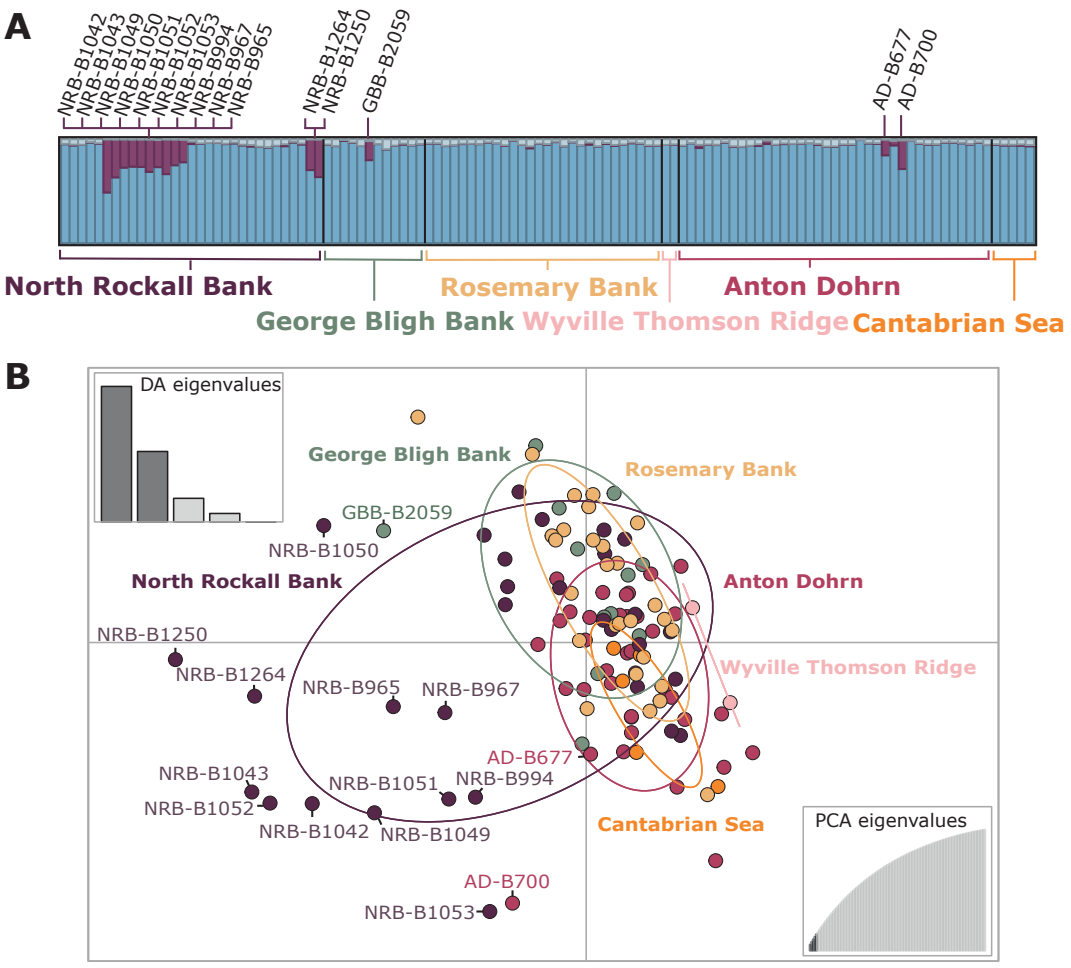

Fig. 6. (A). Individual genotype assignment to clusters (*k*) as inferred by STRUCTURE based on SNPs obtained from RADseq for the dataset only including *Eunice norvegica* specimens with $k = 3$. Each vertical bar represents an individual whereas each color a different genetic cluster (*k*). (B). DAPC of the same dataset grouping samples per location: North Rockall bank (purple), George Bligh Bank (green), Rosemary Bank (yellow), Wyville Thomson Ridge (pink), Anton Dohrn (red) and Cantabrian Sea (orange). (For interpretation of the references to colour in this figure legend, the reader is referred to the web version of this article.)

Table 4
Pairwise *Fst* values based on SNPs obtained from RADseq for samples of *Eunice norvegica* grouped in six locations. Significant values ($p > 0.05$) in bold.

	Anton Dohrn	Cantabrian Sea	George Bligh Bank	North Rockall Bank	Rosemary Bank	Wyville Thomson Ridge
Anton Dohrn	–	**0.008**	**0.009**	**0.018**	**0.004**	0.071
Cantabrian Sea	**0.008**	–	**0.018**	**0.029**	**0.022**	0.065
George Bligh Bank	**0.009**	**0.018**	–	**0.028**	**0.005**	0.077
North Rockall Bank	**0.018**	**0.029**	**0.028**	–	**0.022**	0.100
Rosemary Bank	**0.004**	**0.022**	**0.005**	**0.022**	–	0.065
Wyville Thomson Ridge	0.071	0.065	0.077	0.100	0.065	–

E. philocorallia by Buchanan (1893) and this study, despite being a relatively short distance apart geographically, raises questions on whether *E. philocorallia* is a facultative or obligate symbiont with deep-water corals, the extent of niche overlap with *E. norvegica,* and the constancy of depth distribution and host associations over time. Further sampling across the Atlantic and across a broader depth range may help resolve this in the future.

4.2. Integrative species delimitation

A combined approach using three genetic markers (*16S*, *18S* and *COI*) and morphological characters was sufficient to resolve the different species studied here. As a result of past inconsistencies of molecular and morphological data inside the genus *Eunice*, the genera *Leodice* and *Nicidion* were resurrected by Zanol et al. (2014) to resolve the polyphyletic structure previously observed in the group (Zanol et al., 2010). Since we found *E.* cf. *nicidioformis* and *Eunice pennata* (Müller, 1776) within a well-supported clade with other members of the genus *Leodice*, we suggest that these two species should be transferred to *Leodice*. This possibility is further supported by previous suggestions that both *Leodice* and *Nicidion* may be significantly bigger genera than currently recognized, because of longstanding taxonomic challenges that have historically grouped many divergent species under the genus *Eunice* (Zanol et al., 2020, 2021). Although there are currently no distinct characters

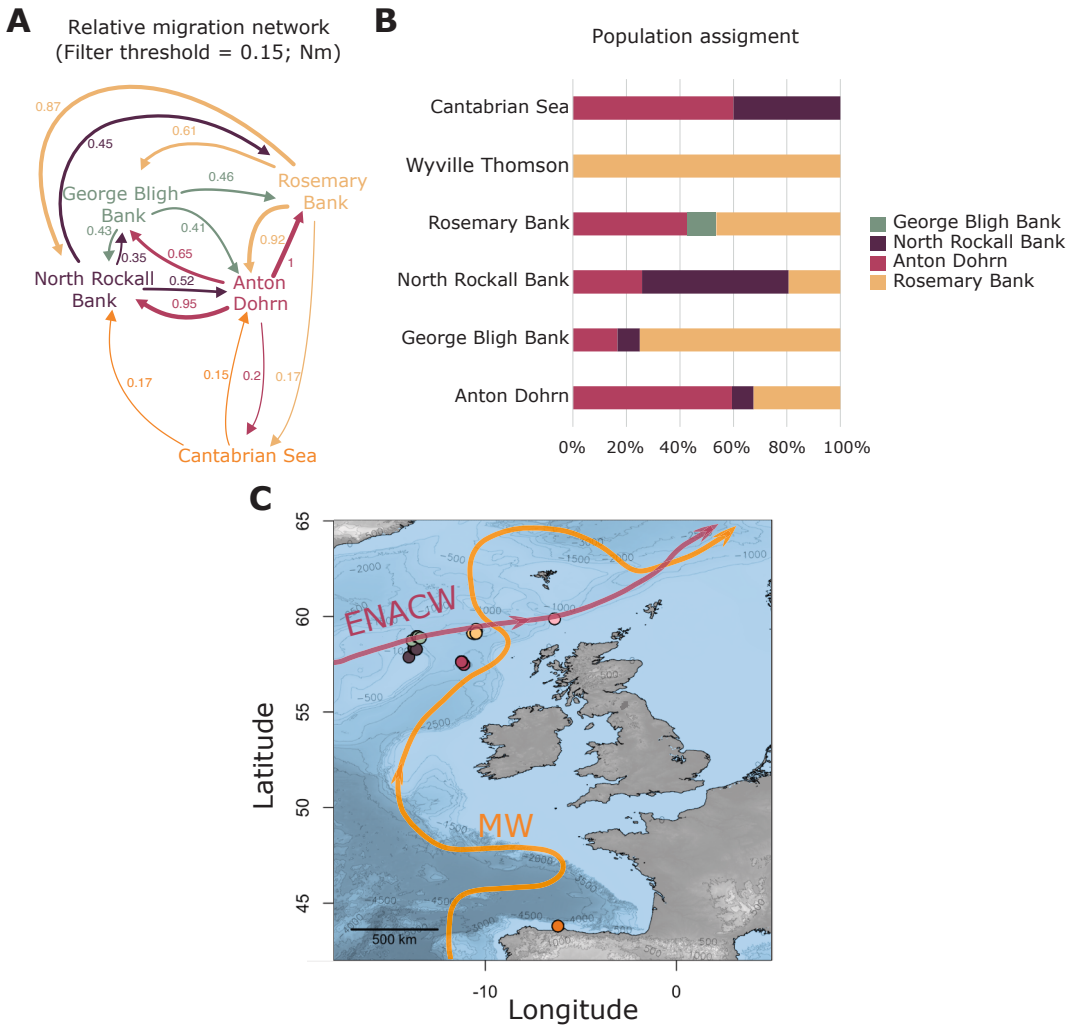

Fig. 7. (A). Contemporary migration observed for *Eunice norvegica* between the different sampling locations based on SNPs obtained from RADseq. Number of migrants (*Nm*) method with no bootstrapping and filter threshold of 0.15. (B). Population assignment of individuals of *E. norvegica.* Each color represents a different sampling location. (C). Predominant oceanographic currents in the NE Atlantic (ENACW = North Atlantic Central Water; MW = Mediterranean Water).

that uniquely define the morphology of the genus *Leodice*, Zanol et al. (2014) proposed several distinguishing morphological traits, suggesting that the presence of just one of these characteristics may be enough for the inclusion in this genus. These features are consistent with several morphological characters reported for *E.* cf. *nicidioformis*, including branchiae appearing as simple filaments and articulated prostomial appendages. In addition, the aciculae observed were dark (Fig. 3C), which agrees with the redescription provided by Fauchald (1992) and represents another character commonly associated with *Leodice*. This information together with the described phylogenetic positioning of the species thus provides evidence that eventually *E.* cf. *nicidioformis* should be transferred to the genus *Leodice*. A more detailed review of broader morphological features, which could not be assessed in the present study, is necessary to confirm the change of genus of this species.

Eunice norvegica and *E. philocorallia* appeared as two closely related species, belonging to two different well-supported sister clades, with limited genetic distance between these two clades (11% *COI*; 4% *18S*), suggesting a relatively recent separation of both species (Fig. 2; Supplementary Data 2). Given their shared distribution and morphological similarities, only distinguishable by the arrangement of the teeth forming the compound falciger (Fig. 3D-E) and the form of the parapodial lobes (Fig. 3A-B), clarifying species boundaries between them is particularly relevant. Our phylogenetic results using traditional markers are in accordance with the RADseq analysis, confirming that *E. philocorallia* and *E. norvegica* are separate species, with no signs of hybridization between them (Fig. 5). However, due to limited sampling and the uniform collection depth *of E. philocorallia*, other evolutionary patterns may remain undetected between these species.

4.3. Genetic and genomic connectivity in Eunicidae

Our *16S* haplotype network analysis showed no evidence of genetic structure in *E. norvegica* despite comparing individuals separated by ca. 2,000 km (Fig. 4A). Comparable results were observed for the RADseq approach, where *E. norvegica* individuals presented a similar genetic signature among the different locations and no clear genetic structure was observed (Fig. 6), thus indicating that *E. norvegica* specimens studied here form a broadly panmictic population spanning from the Cantabrian Sea up to the United Kingdom. This was further corroborated by the low observed heterozygosity (Table 3) and low pairwise *Fst* values (Table 4), indicating similar allele frequencies across different sampling locations, consistent with shared common ancestry and limited genetic differentiation, and supporting a largely homogeneous population structure. Our results were similar to those observed for *E. norvegica* in a study also using a RADseq approach, revealing a genetic homogeneity when comparing samples from the Bay of Biscay and Iceland, and only detecting a genetic break when comparing samples from the Atlantic basin with those from the Mediterranean Sea (Boavida et al., 2019).

Individuals of *E.* cf. *nicidioformis* collected from the clustered sampling stations in the Cantabrian Sea showed almost identical haplotypes (Fig. 4C), and limited genetic diversity (Table 2), indicating high connectivity; a pattern consistent with other deep-sea species exhibiting limited genetic structuring at similar depths and distances (Busch et al., 2021).

Long-distance genetic connectivity over thousands of kilometers is a widely reported phenomenon in deep-sea invertebrate fauna inhabiting similar depths or water masses (Taylor and Roterman, 2017). This is especially true for organisms with a planktotrophic larval stage, since these larvae are able to feed in the water column for many weeks or even months and are capable to disperse passively through prevalent oceanographic currents (Cowen and Sponaugle, 2009; Gary et al., 2020). However, eunicids appear to produce lecithotrophic larvae (Zanol et al., 2021), which might confer them more limited dispersal capabilities than species employing planktotrophic larval dispersal (Modica et al., 2017). The inferred long-distance connectivity in *E. norvegica* may therefore be explained by predominantly northward-flowing oceanographic currents in the region, together with the relatively high abundance of CWC habitats in the NE Atlantic (Arnaud-Haond et al., 2017; Schröder-Ritzrau et al., 2005), functioning as dispersal stepping stones (Saura et al., 2014) and facilitating gene flow across distances of hundreds of kilometers. Indeed, the features where these corals often occur are associated with enhanced hydrodynamic activity (Lim et al., 2020), as CWCs preferentially occur in exposed settings, on elevated seabed features, or in areas where currents are locally intensified by topography (Freiwald, et al., 1999; Genin et al., 1986), something that might enhance the dispersal abilities of *E. norvegica*. In the NE Atlantic, the principal water masses that might be affecting larval dispersal and therefore genetic connectivity among the locations where we collected *E. norvegica* are: (i) the Eastern North Atlantic Central Water (ENACW), in the upper layer, which forms in the inter-gyre region and flows northwards to the United Kingdom; and (ii) the Mediterranean Water (MW), which originates in the intermediate layer after passing through the Gibraltar Strait. The MW mixes with the ENACW, with one of its branches flowing northward along the Iberian Peninsula toward the Norwegian Sea (Jia et al., 2007; Liu and Tanhua, 2021; Reid, 1979) (Fig. 7C). Most of our samples were collected below 500 m, leaving the MW current as the main driver for larval transport, given its depth range of 500 to 1,500 m. This current might be facilitating the lecithotrophic larval dispersal from the Cantabrian Sea to the area of the Wyville Thomson Ridge, promoting gene flow and homogenizing genetic structure across the individuals of these locations, although this remains a hypothesis that would benefit from future biophysical modelling. However, lack of genetic structure could also reflect a synergistic effect between historical and contemporary processes. The widespread negative Tajima's *D* values observed for this species (Table 2) could suggest a rapid post-glacial population expansion and recent colonization across the Northeast Atlantic (Maggs et al., 2008), establishing a homogeneous baseline that is continuously maintained by ongoing larval dispersal.

The lack of vertical genetic structure for *E. norvegica* in this study could be indicative of larvae capable of vertical movement in the water column, as has been demonstrated for its symbiont *D. pertusum* (Strömberg and Larsson, 2017). Vertical movement in the water column has been shown to generally increase dispersal by up to 100 times (Gary et al., 2020), possibly explaining this high connectivity between samples collected within a wide bathymetric range (190–1,230 m). However, depth is also a potential factor influencing genetic structure, as strong and consistent ecological gradients across bathymetric ranges can generate genetic divergence in marine populations (Jennings et al., 2013; Taboada et al., 2025; France and Kocher, 1996). In the case of *E. norvegica*, most samples were collected shallower than 1,000 m (Table 1), and previous studies in the NE Atlantic have detected genetic discontinuities between populations occurring above and below 1,300 m isobath not only in *D. pertusum* but also in deep-water sponges (Morrison et al., 2011; Taboada et al., 2025). Further studies should examine *E. norvegica* samples at depths below 1,300 m to evaluate the presence of a possible genetic break at these depths.

Similar patterns of long-distance connectivity have also been reported in the cold-water coral *D. pertusum* (Weinnig et al., 2024), the principal host of *E. norvegica* in this study. This coral produces planktotrophic larvae capable of surviving in the water column for up to three months, providing substantial potential for long-distance dispersal via ocean currents (Strömberg and Larsson, 2017). The use of biophysical modeling for estimating larval dispersal for the coral confirmed strong connections between canyons on the continental slope off New England southwestwards towards Cape Hatteras, separated by approximately 1,000 km (Guy, 2024). Ross et al. (2017) further highlighted Anton Dohrn and Rockall Bank as key nodes within the Northeast Atlantic MPA network, functioning as both sources and sinks. A previous genetic study on *D. pertusum* using microsatellite data revealed a panmictic population in the NE Atlantic, with a genetic break near the New England Seamounts (Morrison et al., 2011), while a more recent study using a RADseq approach also identified a panmictic population when comparing samples from the Bay of Biscay up to Iceland (Boavida et al., 2019). Our migration analyses for *E. norvegica* reflect these trends, revealing substantial bidirectional migration among sampling sites within the United Kingdom except for Wyville Thomson Ridge (possibly due to low sample size) and between the United Kingdom and the Cantabrian Sea (Fig. 7A–B). These support the hypothesis that *D. pertusum* and *E. norvegica* share long-distance connectivity patterns across their distribution in the Northeast Atlantic Ocean despite having larvae with a different dispersal capacity.

The long-distance genetic connectivity observed in *E. norvegica* contrasts with findings from a recent study of the deep-water sponge *Phakellia ventilabrum* (Linnaeus, 1767), which identified a clear genetic break between populations in the Cantabrian Sea and those in the NE Atlantic (Taboada et al., 2023). Although this sponge is thought to exhibit lecithotrophic larvae or direct development (Koutsouveli et al., 2022), the contrasting connectivity patterns between these taxa, despite their occurrence in the same region, suggest that larval dispersal capacity may be more limited in *P. ventilabrum* than in *E. norvegica*. Additionally, the distribution of *P. ventilabrum* is more spatially fragmented than that of the coral hosts of *E. norvegica*, which may further constrain connectivity (Davies et al., 2008; Sánchez et al., 2009). Consequently, connectivity patterns within the same geographic region may differ substantially among species, even where dispersal potential is broadly comparable. This variability should be considered when designing conservation and management strategies.

Despite the overall genetic homogeneity observed among the *E. norvegica* samples analysed here, some individuals from the North Rockall Bank, George Bligh Bank, and Anton Dohrn Seamount exhibited a certain degree genetic introgression (Fig. 6). To further explore this pattern, depth was assessed as a potential factor shaping genetic structure, as genetic divergence in marine populations often increases across bathymetric gradients (France & Kocher, 1996; Jennings et al., 2013). Depth does not appear to explain this pattern, as haplotypes in the *16S* network were shared across multiple depth ranges (Fig. 4B), and individuals showing introgression were collected from different depths. Host association does not account for this signal either, as introgressed individuals were found on both *D. pertusum* and *M. oculata* (Supplementary Data 1). Instead, these introgression patterns may reflect connectivity with unsampled and genetically differentiated populations beyond the geographic scope of this study. *Eunice norvegica* has a broad distribution that closely follows that of its principal host, *D. pertusum*, raising the possibility of gene flow from populations located elsewhere in the NE Atlantic or adjacent regions. Future studies incorporating broader geographic coverage and greater depth ranges will be necessary to determine the origin and extent of this introgression.

5. Conclusions

This study successfully characterized the diversity and connectivity patterns of eunicid polychaetes in the Northeast Atlantic, identifying four species and revealing marked differences between the closely related *Eunice norvegica* and *Eunice philocorallia*. Our records tentatively assigned to *Eunice* cf. *nicidioformis* and *Leodice* cf. *antarctica* should be treated with caution, as they may represent undescribed taxa requiring further taxonomic investigation. The panmictic population structure of *E. norvegica* across thousands of kilometers suggests extensive connectivity facilitated by oceanographic currents and stepping-stone habitats provided by its main coral host *Desmophyllum pertusum*. Although depth is commonly considered a key driver of genetic differentiation in deep-sea organisms (Taylor and Roterman, 2017), the genetic admixture observed in some individuals was not associated with depth, suggesting more complex population dynamics. Overall, these findings improve our understanding of deep-sea connectivity processes and highlight the importance of preserving habitat networks that sustain gene flow and population resilience. Future studies integrating broader geographic, taxonomic, and genomic sampling will be essential to further resolve taxonomic inconsistencies and population structure in Northeast Atlantic eunicids.

Funding sources

This study was performed with the funding organization Fundación Biodiversidad (granted to S.T.). S.T. received funding from the grant PID2020-117115GA-I00 funded by MCIN/AEI/https://doi.org/10.13039/501100011033 and from the grant CNS2023-144572 and by the Ramón y Cajal grant RYC2021-03152-I, funded by the MCIN/AEI/https://doi.org/10.13039/501100011033 and the European Union «NextGenerationEU»/PRTR». C.G.S. received funding from the grant PIPF-2023/ECO-29837 funded by Comunidad Autónoma de Madrid (CAM). Collection and sequencing of specimens from around the United Kingdom was funded as part of the NERC DeepLinks project (NE/K011855/1 and NE/K013513/1) (granted to K.H. and A.R).

CRediT authorship contribution statement

Carlota Gracia-Sancha: Writing – original draft, Visualization, Software, Investigation, Formal analysis, Data curation. **Nicolai Roterman:** Writing – review & editing, Resources, Investigation, Data curation, Conceptualization. **Michelle L. Taylor:** Writing – review & editing, Resources, Conceptualization. **Kerry L. Howell:** Writing – review & editing, Resources, Project administration, Conceptualization. **Alex D. Rogers:** Writing – review & editing, Resources, Project administration, Conceptualization. **Sofía Ruiz-Cano:** Writing – review & editing, Visualization, Formal analysis. **Sergi Taboada:** Writing – review & editing, Visualization, Supervision, Resources, Project administration, Investigation, Funding acquisition, Conceptualization.

Declaration of competing interest

The authors declare that they have no known competing financial interests or personal relationships that could have appeared to influence the work reported in this paper.

Acknowledgments

We send out deepest thanks to the staff and participants of RRS *James* Cook (JC136) and the technical support of the remotely operated vehicle (ROV) *Isis* staff too; This was part of the NERC-funded DeepLinks project (NE/K011855/1 and NE/K013513/1). The authors would like to thank the molecular laboratory at the MNCN for allowing us to carry out the necessary protocols for the study, as well as the High-resolution 3D Microscopy Laboratory of MNCN for taking the SEM photos. We would also like to thank the Natural History Museum (London) for allowing us to use their cluster for data analysis. Three anonymous reviewers greatly improved a previous version of the manuscript.

Appendix A. Supplementary data

Supplementary data to this article can be found online at https://doi.org/10.1016/j.ympev.2026.108697.

Data availability

Data will be made available on request.

References

Alcala, N., Goudet, J., Vuilleumier, S., 2014. On the transition of genetic differentiation from isolation to panmixia: what we can learn from G S T and D. Theor. Popul Biol. 93, 75–84. https://doi.org/10.1016/j.tpb.2014.02.003.

Almón, B., Garrido, M., Meseguer, C., Arcos, J.M., Martín, V., Pantoja, J., Consuegra, E., 2014. Espacio Marino del Oriente y Sur de Lanzarote-Fuerteventura. Proyecto LIFE + INDEMARES. Fundación Biodiversidad del Ministerio de Agricultura, Alimentación y Medio Ambiente.

Arnaud-Haond, S., Van den Beld, I.M.J., Becheler, R., Orejas, C., Menot, L., Frank, N., Grehan, A., Bourillet, J.F., 2017. Two "pillars" of cold-water coral reefs along Atlantic European margins: Prevalent association of Madrepora oculata with Lophelia pertusa, from reef to colony scale. Deep Sea Res 2 Top Stud Oceanogr 145, 110–119. Doi: 10.1016/j.dsr2.2015.07.013.

Augener, H., 1922. Ueber litorale Polychaeten von Westindien. Sitzungsberichte der Gesellschaft Naturforschender Freunde zu Berlin 3–5, 38–53.

Baird, W., 1869. Remarks on several genera of annelides, belonging to the group Eunicea, with a notice of such species as are contained in the collection of the British Museum, and a description of some others hitherto undescribed. Journal of the Linnean Society of London 10, 341–361.

Beaumont, M.A., Nichols, R.A., 1996. Evaluating loci for use in the genetic analysis of population structure. Proc. R. Soc. B Biol. Sci. 263, 1619–1626. https://doi.org/10.1098/rspb.1996.0237.

Becker, B.J., Levin, L.A., Fodrie, F.J., Mcmillan, P.A., 2007. Complex larval connectivity patterns among marine invertebrate populations. Procedings of the National Academy of Sciences of the United States of America 104, 3267–3272.

Benestan, L., Gosselin, T., Perrier, C., Sainte-Marie, B., Rochette, R., Bernatchez, L., 2015. RAD genotyping reveals fine-scale genetic structuring and provides powerful population assignment in a widely distributed marine species, the American lobster (Homarus americanus). Mol. Ecol. 24, 3299–3315. https://doi.org/10.1111/mec.13245.

Benjamini, Y., Hochberg, Y., 1995. Controlling the False Discovery Rate-a Practical and Powerful Approach to Multiple Testing. Article in Journal of the Royal Statistical Society Series B. https://doi.org/10.2307/2346101.

Boavida, J, Becheler, R., Addamo, A.M., Sylvestre, F., Arnaud-Haond, S., 2019. Past, Present and Future Connectivity of Mediterranean Cold-Water Corals: Patterns, Drivers and Fate in a Technically and Environmentally Changing World, in: Orejas, C., Jiménez, C. (Eds.), Mediterranean Cold-Water Corals: Past, Present and Future. Springer, Cham.

Brown, S.D.J., Collins, R.A., Boyer, S., Lefort, M.-C., Malumbres-Olarte, J., Vink, C.J., Cruickshank, R.H., 2012. Spider: an R package for the analysis of species identity and evolution, with particular reference to DNA barcoding. Mol. Ecol. Resour. 12, 562–565. https://doi.org/10.1111/j.1755-0998.2011.03108.x.

Buchanan, F., 1893. Report on polychaets collected during the Royal Dublin Society's survey off the west coast of Ireland. Pt. I. Deep water forms. Sci. Proc. R. Dublin Soc. 8, 169–179.

Buhl-Mortensen, L., Mortensen, P.B., 2004. Symbiosis in deep-water corals. Symbiosis 37, 33–61.

Buhl-Mortensen, L., Vanreusel, A., Gooday, A.J., Levin, L.A., Priede, I.G., Buhl-Mortensen, P., Gheerardyn, H., King, N.J., Raes, M., 2010. Biological structures as a source of habitat heterogeneity and biodiversity on the deep ocean margins. Mar. Ecol. 31, 21–50. https://doi.org/10.1111/j.1439-0485.2010.00359.x.

Buhl-Mortensen, P., 2017. Coral reefs in the Southern Barents Sea: habitat description and the effects of bottom fishing. Mar. Biol. Res. 13, 1027–1040. https://doi.org/10.1080/17451000.2017.1331040.

Busch, K., Taboada, S., Riesgo, A., Koutsouveli, V., Ríos, P., Cristobo, J., Franke, A., Getzlaff, K., Schmidt, C., Biastoch, A., Hentschel, U., 2021. Population connectivity of fan-shaped sponge holobionts in the deep Cantabrian Sea. Deep Sea Res 1 Oceanogr Res Pap 167. Doi: 10.1016/j.dsr.2020.103427.

Cairns, S.D., 2007. Deep-water corals: an overview with special reference to diversity and distribution of Deep-water scleractinian corals, BULLETIN OF MARINE SCIENCE.

Capel, K.C.C., Leocorny, P., de Mello Carpes, R., Kitahara, M.V., Zilberberg, C., 2025. High genetic connectivity of the two main cold-water scleractinian framework engineers from the Southwestern Atlantic. Deep Sea Res 1 Oceanogr Res Pap 226. Doi: 10.1016/j.dsr.2025.104606.

Carlier, A., Le Guilloux, E., Olu, K., Sarrazin, J., Mastrototaro, F., Taviani, M., Clavier, J., 2009. Trophic relationships in a deep Mediterranean cold-water coral bank (Santa Maria di Leuca, Ionian sea). Mar. Ecol. Prog. Ser. 397, 125–137. https://doi.org/10.3354/meps08361.

Castresana, J., 2000. Selection of Conserved Blocks from Multiple Alignments for their use in Phylogenetic Analysis. Mol. Biol. Evol. 17, 540–552.
Catchen, J., Hohenlohe, P.A., Bassham, S., Amores, A., Cresko, W.A., 2013. Stacks: an analysis tool set for population genomics. Mol. Ecol. 22, 3124–3140. https://doi.org/10.1111/mec.12354.
Cathalot, C., Van Oevelen, D., Cox, T.J.S., Kutti, T., Lavaleye, M., Duineveld, G., Meysman, F.J.R., 2015. Cold-water coral reefs and adjacent sponge grounds: Hotspots of benthic respiration and organic carbon cycling in the deep sea. Front. Mar. Sci. 2. https://doi.org/10.3389/fmars.2015.00037.
Clement, M., Posada, D., Crandall, K.A., 2000. TCS: a computer program to estimate gene genealogies. Mol. Ecol. 9, 1657–1659. https://doi.org/10.1046/j.1365-294X.2000.01020.x.
Colgan, D.J., Hutchings, P.A., Brown, S., 2001. Phylogenetic relationships within the Terebellomorpha. J. Mar. Biol. Assoc. U. K. 81, 765–773. https://doi.org/10.1017/S002531540100457X.
Costello, M.J., Mccrea, M., Freiwald, André, Lundälv, T., Jonsson, L., Bett, B.J., Van Weering, T.C.E., De Haas, H., Roberts, J Murray, Allen, D., 2005. Role of cold-water *Lophelia pertusa* coral reefs as fi sh habitat in the NE Atlantic, in: Freiwald, A., Roberts, J.M. (Eds.), Cold-Water Corals and Ecosystems. Springer, Berlin, pp. 771–805. Doi: Doi: 10.1007/3-540-27673-4_41.
Cowen, R.K., Gawarkiewicz, G., Pineda, J., Thorrold, S.R., Werner, F.E., 2007. Population connectivity in marine systems: an overview. Oceanography 20, 14–21. https://doi.org/10.5670/oceanog.2007.26.
Cowen, R.K., Sponaugle, S., 2009. Larval dispersal and marine population connectivity. Ann. Rev. Mar. Sci. https://doi.org/10.1146/annurev.marine.010908.163757.
Dahl, M.P., Pereyra, R.T., Lundälv, T., André, C., 2012. Fine-scale spatial genetic structure and clonal distribution of the cold-water coral *Lophelia pertusa*. Coral Reefs 31, 1135–1148. https://doi.org/10.1007/s00338-012-0937-5.
Darriba, D., Taboada, G.L., Doallo, R., Posada, D., 2012. JModelTest 2: more models, new heuristics and parallel computing. Nat. Methods. https://doi.org/10.1038/nmeth.2109.
Davies, A.J., Wisshak, M., Orr, J.C., Roberts, J.M., 2008. Predicting suitable habitat for the cold-water coral *Lophelia pertusa* (Scleractinia). Deep Sea Res. Part I 55 (8), 1048–1062. https://doi.org/10.1016/j.dsr.2008.04.010.
De Clippele, L.H., Buhl-Mortensen, P., Buhl-Mortensen, L., 2015. Fauna associated with cold water gorgonians and sea pens. Cont. Shelf Res. 105, 67–78. https://doi.org/10.1016/j.csr.2015.06.007.
De León-González, J.A., Díaz, V., 2006. Eunicidae (Annelida: Polychaeta) associated with Phragmathopoma caudata Morch, 1863 and some coral reefs from Veracruz, Gulf of Mexico. Sci Mar 70. Doi: Doi: 10.3989/scimar.2006.70s391.
De Santo, E.M., Jones, P.J.S., 2007. The Darwin Mounds: from undiscovered coral to the development of an offshore marine protected area regime. Bull. Mar. Sci. 81 (1), 147–156.
Duncan, P.M., 1873. A description of the Madreporaria dredged up during the Expeditions of H.M.S. “porcupine” in 1869 and 1870. Transactions of the Zoological Society of London.
Earl, D.A., vonHoldt, B.M., 2012. STRUCTURE HARVESTER: a website and program for visualizing STRUCTURE output and implementing the Evanno method. Conserv. Genet. Resour. 4, 359–361. https://doi.org/10.1007/s12686-011-9548-7.
Edler, D., Klein, J., Antonelli, A., Silvestro, D., 2021. raxmlGUI 2.0: a graphical interface and toolkit for phylogenetic analyses using RAxML. Methods Ecol. Evol. 12, 373–377. https://doi.org/10.1111/2041-210X.13512.
Eilertsen, M.H., Georgieva, M.N., Kongsrud, J.A., Linse, K., Wiklund, H., Glover, A.G., Rapp, H.T., 2018. Genetic connectivity from the Arctic to the Antarctic: Sclerolinum contortum and Nicomache lokii (Annelida) are both widespread in reducing environments. Sci. Rep. 8. https://doi.org/10.1038/s41598-018-23076-0.
Excoffier, L., Lischer, H.E.L., 2010. Arlequin suite ver 3.5: a new series of programs to perform population genetics analyses under Linux and Windows. Mol. Ecol. Resour. 10, 564–567. https://doi.org/10.1111/j.1755-0998.2010.02847.x.
Fauchald, K., 1992. A Review of the Genus Eunice (Polychaeta: Eunicidae) Based upon Type Material. Smithsonian contributions to zoology , Washington, D.C. .
Fauchald, K., Granados-Barba, A., Solís-Weiss, V., 2009. Polychaeta (Annelida) of the Gulf of Mexico, in: Tunnell, J.W., Camp, D.K. (Eds.), Gulf of Mexico Origin, Waters, and Biota: Biodiversity. Texas A&M University Press, College Station, Texas, pp. 751–788.
Foll, M., Gaggiotti, O., 2008. A genome-scan method to identify selected loci appropriate for both dominant and codominant markers: a Bayesian perspective. Genetics 180, 977–993. https://doi.org/10.1534/genetics.108.092221.
Fosså, J.H., Mortensen, P.B., Furevik, D.M., 2002. The deep-water coral *Lophelia pertusa* in norwegian waters: distribution and fishery impacts. Hydrobiologia.
France, S.C., Kocher, T.D., 1996. Geographic and bathymetric patterns of mitochondria116S rRNA sequence divergence among deep-sea amphipods, Eurythenes gryllus, Marine Biology. Springer-Verlag.
Freiwald, A., Wilson, J.B., Henrich, R., 1999. Grounding Pleistocene icebergs shape recent deep-water coral reefs. Sed. Geol. 125, 1–8. https://doi.org/10.1016/S0037-0738(98)00142-0.
Gary, S.F., Fox, A.D., Biastoch, A., Roberts, J.M., Cunningham, S.A., 2020. Larval behaviour, dispersal and population connectivity in the deep sea. Sci. Rep. 10. https://doi.org/10.1038/s41598-020-67503-7.
Genin, A., Dayton, P., Lonsdale, S.F.N., 1986. Corals on seamount peaks provide evidence of current acceleration over deep-sea topography. Nature 322, 59–61. https://doi.org/10.1038/322059a0.
Gil, J.C., 2011. The European Fauna of Annelida Polychaeta (I). Universidade de Lisboa, Lisboa.
Gillet, P., Dauvin, J.C., 2003. Polychaetes from the Irving, Meteor and Plato seamounts, North Atlantic ocean: Origin and geographical relationships. J. Mar. Biol. Assoc. U. K. 83, 49–53. https://doi.org/10.1017/s0025315403006799h.
Giribet, G., Edgecombe, G.D., Wheeler, W.C., Babbitt, C., 2002. Phylogeny and systematic position of opiliones: a combined analysis of chelicerate relationships using morphological and molecular data. Cladistics 18, 5–70. https://doi.org/10.1006/clad.2001.0185.
Goff-Vitry, M.C.L., Pybus, O.G., Rogers, D., 2004. Genetic structure of the deep-sea coral *Lophelia pertusa* in the northeast Atlantic revealed by microsatellites and internal transcribed spacer sequences. Mol. Ecol. 13, 537–549. https://doi.org/10.1046/j.1365-294X.2004.02079.x.
Gravina, M.F., Pierri, C., Mercurio, M., Nonnis Marzano, C., Giangrande, A., 2021. Polychaete diversity related to different mesophotic bioconstructions along the southeastern italian coast. Diversity (basel) 13. https://doi.org/10.3390/d13060239.
Grehan, A., Unnithan, V., Wheeler, A., Monteys, X., Beck, T., Wilson, M., Guinan, J., Foubert, A., Klages, M., Thiede, J., 2004. Evidence of major fisheries impact on cold-water corals in the deep waters off the Porcupine Bank, west coast of Ireland: are interim management measures required? ICES CM 2004/AA:07. https://doi.org/10.17895/ices.pub.25349143.
Grube, A.E., 1856. Annulata Örstediana. Enumeratio Annulatorum, quae in itinere per Indiam occidentalem et Americam centralem annis 1845-1848 suscepto legit cl. A.S. Örsted, adjectis speciebus nonnullis a cl. H. Kröyero in itinere ad Americam meridionalem collectis. [Part 1]. Videnskabelige Meddelelser fra Dansk naturhistorisk Forening i Köbenhavn 1854–1856, 56.
Guy, G., 2024. Population Connectivity of *Lophelia pertusa* (=*Desmophyllum pertusum*). In the North Atlantic Ocean. Present-Day Connections and Future Predictions.
Guy, G., Metaxas, A., Nizinski, M., Wang, Z., 2025. Stable connections in the deep sea: Temporally consistent larval pathways for the deep-sea coral, *Lophelia pertusa* (=*Desmophyllum pertusum*) in the Northwest Atlantic Ocean. Deep Sea Res 1 Oceanogr Res Pap 218. Doi: 10.1016/j.dsr.2025.104462.
Haddon, A.C., 1895. Branched worm-tubes and Acrozoanthus. Sci. Proc. R. Dublin Soc. 8, 344–346.
Hartman, O., 1944. Polychaetous Annelids. Part V. Eunicea. Allan Hancock Pacific expeditions v.10 (1944-1947), 118–121.
Hernández-Alcántara, P., Cruz-Pérez, I.N., Solís-Weiss, V., 2019. Composition and diversity patterns of Eunicida and Amphinomida (Annelida) associated to dead coral in the Chinchorro Bank Biosphere Reserve, Caribbean Sea. J. Mar. Biol. Assoc. U. K. 99, 1547–1555. https://doi.org/10.1017/S0025315419000675.
Hickson, S.J., 1907. The Alcyonaria, Antipatharia, and Madreporaria collected by the“ Huxley” from the North Side of the Bay of Biscay in August, 1906. J. Mar. Biol. Assoc. U. K. 8, 6–14. https://doi.org/10.1017/S0025315400043708.
Hohenlohe, P.A., Amish, S.J., Catchen, J.M., Allendorf, F.W., Luikart, G., 2011. Next-generation RAD sequencing identifies thousands of SNPs for assessing hybridization between rainbow and westslope cutthroat trout. Mol. Ecol. Resour. 11, 117–122. https://doi.org/10.1111/j.1755-0998.2010.02967.x.
Jakobsson, M., Rosenberg, N.A., 2007. CLUMPP: a cluster matching and permutation program for dealing with label switching and multimodality in analysis of population structure. Bioinformatics 23, 1801–1806. https://doi.org/10.1093/bioinformatics/btm233.
Jeffries, D.L., Copp, G.H., Handley, L.L., Håkan Olsén, K., Sayer, C.D., Hänfling, B., 2016. Comparing RADseq and microsatellites to infer complex phylogeographic patterns, an empirical perspective in the Crucian carp, Carassius carassius, L. Mol. Ecol. 25, 2997–3018. https://doi.org/10.1111/mec.13613.
Jenkins, T.L., Stevens, J.R., 2018. Assessing connectivity between MPAs: Selecting taxa and translating genetic data to inform policy. Mar. Policy 94, 165–173. https://doi.org/10.1016/j.marpol.2018.04.022.
Jennings, R.M., Etter, R.J., Ficarra, L., 2013. Population Differentiation and Species Formation in the Deep Sea: the potential Role of Environmental Gradients and Depth. PLoS One 8. https://doi.org/10.1371/journal.pone.0077594.
Jia, Y., Coward, A.C., de Cuevas, B.A., Webb, D.J., Drijfhout, S.S., 2007. A model analysis of the behavior of the Mediterranean water in the North Atlantic. J. Phys. Oceanogr. 37, 764–786. https://doi.org/10.1175/JPO3020.1.
Jombart, T., Devillard, S., Balloux, F., 2010. Discriminant analysis of principal components: a new method for the analysis of genetically structured populations. BMC Genet. 11. https://doi.org/10.1186/1471-2156-11-94.
Katoh, K., Rozewicki, J., Yamada, K.D., 2019. MAFFT online service: multiple sequence alignment, interactive sequence choice and visualization. Brief. Bioinform. 20, 1160–1166. https://doi.org/10.1093/bib/bbx108.
Kazanidis, G., Henry, L.A., Roberts, J.M., 2021. Hidden structural heterogeneity enhances marine hotspots’ biodiversity. Coral Reefs 40, 1615–1630. Doi: 10.1007/s00338-021-02114-w.
Kearse, M., Moir, R., Wilson, A., Stones-Havas, S., Cheung, M., Sturrock, S., Buxton, S., Cooper, A., Markowitz, S., Duran, C., Thierer, T., Ashton, B., Meintjes, P., Drummond, A., 2012. Geneious basic: an integrated and extendable desktop software platform for the organization and analysis of sequence data. Bioinformatics 28, 1647–1649. https://doi.org/10.1093/bioinformatics/bts199.
Keenan, K., Mcginnity, P., Cross, T.F., Crozier, W.W., Prodöhl, P.A., 2013. DiveRsity: an R package for the estimation and exploration of population genetics parameters and their associated errors. Methods Ecol. Evol. 4, 782–788. https://doi.org/10.1111/2041-210X.12067.
Kinberg, J.G.H., 1865. Annulata nova. Öfversigt af Königlich Vetenskapsakademiens förhandlingar, Stockholm 21, 559–574.
Koutsouveli, V., Balgoma, D., Checa, A., Hedeland, M., Riesgo, A., Cárdenas, P., 2022. Oogenesis and lipid metabolism in the deep-sea sponge Phakellia ventilabrum (Linnaeus, 1767). Sci. Rep. 12. https://doi.org/10.1038/s41598-022-10058-6.

Lamarck, J.B., 1818. Histoire naturelle des animaux sans vertèbres, 2. Deterville, Paris. https://doi.org/10.5962/bhl.title.40014.
Leigh, J.W., Bryant, D., 2015. POPART: Full-feature software for haplotype network construction. Methods Ecol. Evol. 6, 1110–1116. https://doi.org/10.1111/2041-210X.12410.
Leland, W.P., 1998. A Practical Guide to the Marine Animals of Northeastern North America. New Brunswick, New Jersey & London.
Liline, S., Amin, M., Lestari, U., Corebima Aloysius, D., 2017. The identification of laor worms (Polychaeta) in marine areas of Ambon Island, Mollucas Province, Indonesia based on 16s rRNA gene sequence.
Lim, A., Wheeler, A.J., Price, D.M., O'Reilly, L., Harris, K., Conti, L., 2020. Influence of benthic currents on cold-water coral habitats: a combined benthic monitoring and 3D photogrammetric investigation. Sci. Rep. 10 (1). https://doi.org/10.1038/s41598-020-76446-y.
Linnaeus, C., 1758. Systema naturae per regna tria naturae: secundum classes, ordines, genera, species, cum characteribus, differentiis, synonymis, locis, 10th ed. Impensis Direct.
Linnaeus, C. 1767. Systema naturae per regna tria naturae : secundum classes, ordines, genera, species, cum characteribus, differentiis, synonymis, locis, Editio decima tertia. ed, Systema Naturae. https://doi.org/10.5962/bhl.title.37256.
Liu, M., Tanhua, T., 2021. Water masses in the Atlantic Ocean: characteristics and distributions. Ocean Sci. 17, 463–486. https://doi.org/10.5194/os-17-463-2021.
Luikart, G., England, P.R., Tallmon, D., Jordan, S., Taberlet, P., 2003. The power and promise of population genomics: from genotyping to genome typing. Nat. Rev. Genet. https://doi.org/10.1038/nrg1226.
Maggs, C.A., Castilho, R., Foltz, D., Henzler, C., Jolly, M.T., Kelly, J., Olsen, J., Perez, K. E., Stam, W., Väinölä, R., Viard, F., Wares, J., 2008. Evaluating signatures of glacial refugia for North Atlantic benthic marine taxa. Ecology 89 (Suppl. 11), S108–S122.
Malinsky, M., Trucchi, E., Lawson, D.J., Falush, D., 2018. RADpainter and fineRADstructure: Population Inference from RADseq Data. Mol. Biol. Evol. 35, 1284–1290. https://doi.org/10.1093/molbev/msy023.
Matos, F.L., Aguzzi, J., Company, J.B., Cunha, M.R., 2024. Gone with the stream: Functional connectivity of a cold-water coral at basin scale. Limnol. Oceanogr. 69, 217–231. https://doi.org/10.1002/lno.12444.
Meirmans, P.G., Van Tienderen, P.H., 2004. GENOTYPE and GENODIVE: two programs for the analysis of genetic diversity of asexual organisms. Mol. Ecol. Notes 4, 792–794. https://doi.org/10.1111/j.1471-8286.2004.00770.x.
M'Intosh, W.C., 1903. LXXVI.—Notes from the Gatty Marine Laboratory, St. Andrews.—No. XXIV. Ann. Mag. Nat. Hist. 11, 553–565. https://doi.org/10.1080/00222930308678816.
Modica, M.V., Russini, V., Fassio, G., Oliverio, M., 2017. Do larval types affect genetic connectivity at sea? Testing hypothesis in two sibling marine gastropods with contrasting larval development. Mar. Environ. Res. 127, 92–101. https://doi.org/10.1016/j.marenvres.2017.04.001.
Montgomery, E.M., Hamel, J.F., Mercier, A., 2019. Larval nutritional mode and swimming behaviour in ciliated marine larvae. J. Mar. Biol. Assoc. U. K. https://doi.org/10.1017/S0025315418001091.
Morrison, C.L., Ross, S.W., Nizinski, M.S., Brooke, S., Järnegren, J., Waller, R.G., Johnson, R.L., King, T.L., 2011. Genetic discontinuity among regional populations of *Lophelia pertusa* in the North Atlantic Ocean. Conserv. Genet. 12, 713–729. https://doi.org/10.1007/s10592-010-0178-5.
Mortensen, P.B., 2001. Aquarium observations on the deep-water coral *Lophelia pertusa* (L., 1758) (scleractinia) and selected associated invertebrates. Ophelia 54, 83–104. https://doi.org/10.1080/00785236.2001.10409457.
Mueller, C.E., Lundälv, T., Middelburg, J.J., van Oevelen, D., 2013. The Symbiosis between *Lophelia pertusa* and *Eunice norvegica* Stimulates Coral Calcification and Worm Assimilation. PLoS One 8. https://doi.org/10.1371/journal.pone.0058660.
Müller, O.F., 1776. Zoologiae Danicae Prodromus, seu Animalium Daniae et Norvegiae Indigenarum characters, nomina, et synonyma imprimis popularium. Typis Hallageriis, Havniae 32, 1–282.
Orr, J.C., Fabry, V.J., Aumont, O., Bopp, L., Doney, S.C., Feely, R.A., Gnanadesikan, A., Gruber, N., Ishida, A., Joos, F., Key, R.M., Lindsay, K., Maier-Reimer, E., Matear, R., Monfray, P., Mouchet, A., Najjar, R.G., Plattner, G.K., Rodgers, K.B., Sabine, C.L., Sarmiento, J.L., Schlitzer, R., Slater, R.D., Totterdell, I.J., Weirig, M.F., Yamanaka, Y., Yool, A., 2005. Anthropogenic ocean acidification over the twenty-first century and its impact on calcifying organisms. Nature 437, 681–686. https://doi.org/10.1038/nature04095.
Palumbi, S.R., 1996. Nucleic acids II: the polymerase chain reaction, in: Hillis, D.M., Mable, B.K., Moritz, C. (Eds.), Molecular Systematics. Sinauer, Sunderland, Massachussetts, pp. 205–247.
Paradis, E., 2010. pegas: an R package for population genetics with an integrated–modular approach. Bioinformatics 26, 419–420. https://doi.org/10.1093/bioinformatics/btp696.
Paradis, E., Schliep, K., 2019. ape 5.0: an environment for modern phylogenetics and evolutionary analyses in R. Bioinformatics 35, 526–528. https://doi.org/10.1093/bioinformatics/bty633.
Paris, J.R., Stevens, J.R., Catchen, J.M., 2017. Lost in parameter space: a road map for stacks. Methods Ecol. Evol. 8, 1360–1373. https://doi.org/10.1111/2041-210X.12775.
Pritchard, J.K., Stephens, M., Donnelly, P., 2000. Inference of Population Structure Using Multilocus Genotype Data.
Quatrefages, A., 1866. Histoire naturelle des Annelés marins et d'eau douce. Annélides et Géphyriens. Librarie Encyclopédique de Roret 1.
Quattrini, A.M., Baums, I.B., Shank, T.M., Morrison, C.L., Cordes, E.E., 2015. Testing the depth-differentiation hypothesis in a deepwater octocoral. Proc. R. Soc. B 282, 20150008. https://doi.org/10.1098/rspb.2015.0008.
R Core Team, 2024. R: A language and environment for statistical computing. R Foundation for Statistical Computing, Vienna, Austria. https://www.R-project.org/.
Rambaut, A., 2018. http://tree.bio.ed.ac.uk/software/figtree/ [WWW Document].
Reed, J.K., 2002. Deep-water Oculina coral reefs of Florida: biology, impacts, and management. Hydrobiologia.
Reed, J.K., Koenig, C.C., Shepard, A.N., 2007. Impacts of bottom trawling on a deep-water Oculina coral ecosystem off Florida, BULLETIN OF MARINE SCIENCE.
Reid, J.L., 1979. On the contribution of the Mediterranean Sea outflow to the Norwegian-Greenland Sea. Deep-Sea Res. 26, 1199–1223.
Rex, M.A., Etter, R.J., 2010. Deep-sea biodiversity: pattern and scale. Harvard University Press, Cambridge, Mass; London.
Roberts, J.M., 2005. Reef-aggregating behaviour by symbiotic eunicid polychaetes from cold-water corals: do worms assemble reefs? J. Mar. Biol. Assoc. U. K. 85, 813–819. https://doi.org/10.1017/S0025315405011756.
Roberts, J.M., Cairns, S.D., 2014. Cold-water corals in a changing ocean. Curr. Opin. Environ. Sustain. https://doi.org/10.1016/j.cosust.2014.01.004.
Roberts, J.M., Long, D., Wilson, J.B., Mortensen, P.B., Gage, J.D., 2003. The cold-water coral *Lophelia pertusa* (Scleractinia) and enigmatic seabed mounds along the north-east Atlantic margin: are they related? Mar. Pollut. Bull. 7–20.
Roberts, J.M., Wheeler, A.J., Freiwald, A., Cairns, S.D., 2009. Cold-water corals: The biology and geology of deep-sea coral habitats, Cold-Water Corals: The Biology and Geology of Deep-Sea Coral Habitats. Cambridge University Press. https://doi.org/10.1017/CBO9780511581588.
Rogers, A.D., 1999. The biology of *Lophelia pertusa* (Linnaeus 1758) and other deep-water reef-forming corals and impacts from human activities. Int. Rev. Hydrobiol. 84, 315–406.
Roesti, M., Salzburger, W., Berner, D., 2012. Uninformative polymorphisms bias genome scans for signatures of selection. BMC Evol. Biol. 12. https://doi.org/10.1186/1471-2148-12-94.
Ross, R.E., Nimmo-Smith, W.A.M., Howell, K.L., 2017. Towards 'ecological coherence': Assessing larval dispersal within a network of existing Marine Protected Areas. Deep-Sea Res. Pt. I 126, 128–138. https://doi.org/10.1016/j.dsr.2017.06.004.
Rozas, J., Ferrer-Mata, A., Sanchez-DelBarrio, J.C., Guirao-Rico, S., Librado, P., Ramos-Onsins, S.E., Sanchez-Gracia, A., 2017. DnaSP 6: DNA sequence polymorphism analysis of large data sets. Mol. Biol. Evol. 34, 3299–3302. https://doi.org/10.1093/molbev/msx248.
Sağlam, N., Sarieyyüpoğlu, M., 2008. Eunice norvegica (Polychaeta: Eunicidae) in the Gill of Horse mackerel (Trachurus trachurus). Int. J. Nat. Eng. Sci. 2, 37–39.
Sánchez, F., Serrano, A., Ballesteros, M.G., 2009. Photogrammetric quantitative study of habitat and benthic communities of deep cantabrian Sea hard grounds. Cont. Shelf Res. 29, 1174–1188. https://doi.org/10.1016/j.csr.2009.01.004.
Saura, S., Bodin, Ö., Fortin, M.J., 2014. EDITOR'S CHOICE: Stepping stones are crucial for species' long-distance dispersal and range expansion through habitat networks. J. Appl. Ecol. 51, 171–182. https://doi.org/10.1111/1365-2664.12179.
Schneider, S., Roessli, D., Excoffier, L., 2000. ARLEQUIN ver 2.000. Geneva.
Schröder-Ritzrau, A., Freiwald, A., Mangini, A. (2005). U/Th-dating of deep-water corals from the eastern North Atlantic and the western Mediterranean Sea. In A. Freiwald & J. M. Roberts (Eds.), Cold-water Corals and Ecosystem, 157–172. Springer. Doi: 3-540-24136-1.
Strömberg, S.M., Larsson, A.I., 2017. Larval behavior and longevity in the cold-water coral *Lophelia pertusa* indicate potential for long distance dispersal. Front. Mar. Sci. 4. https://doi.org/10.3389/fmars.2017.00411.
Taboada, S., Díez-Vives, C., Turon, M., Belén Arias, M., Galià-, C., Cárdenas, P., Koutsouveli, V., Correia de Carvalho, F., Davies, A.J., Wang, S., Martín-Huete, M., Roberts, M., Xavier, J.R., Combosch, D., Riesgo, A., 2025. Connectivity and adaptation patterns of the deep-sea ground-forming sponge Geodia hentscheli across its entire distribution. Mol. Biol. Evol. 42. https://doi.org/10.1093/molbev/msaf145.
Taboada, S., Whiting, C., Wang, S., Ríos, P., Davies, A.J., Mienis, F., Kenchington, E., Cárdenas, P., Cranston, A., Koutsouveli, V., Cristobo, J., Rapp, H.T., Drewery, J., Baldó, F., Morrow, C., Picton, B., Xavier, J.R., Arias, M.B., Leiva, C., Riesgo, A., 2023. Long distance dispersal and oceanographic fronts shape the connectivity of the keystone sponge Phakellia ventilabrum in the deep northeast Atlantic. Front. Mar. Sci. 10. https://doi.org/10.3389/fmars.2023.1177106.
Tajima, F., 1989. Statistical method for testing the neutral mutation hypothesis by DNA polymorphism. Genetics 123, 585–595. https://doi.org/10.1093/genetics/123.3.585.
Taylor, M.L., Roterman, C.N., 2017. Invertebrate population genetics across Earth's largest habitat: the deep-sea floor. Mol. Ecol. https://doi.org/10.1111/mec.14237.
Treadwell, A.L., 1906. Polychaetous annelids of the hawaiian Islands collected by the steamer Albatross in 1902. Bulletin of the United States Fish Commission 23, 1145–1181.
Wang, S., Kenchington, E., Murillo, F.J., Lirette, C., Wang, Z., Koen-Alonso, M., Kenny, A., Sacau, M., Pepin, P., 2024. Quantifying the effects of fragmentation of connectivity networks of deep-sea vulnerable marine ecosystems. Divers. Distrib. 30. https://doi.org/10.1111/ddi.13824.
Weinnig, A.M., Aunins, A.W., Salamone, V., Quattrini, A.M., Nizinski, M.S., Morrison, C. L., 2024. Population structure of Desmophyllum pertusum found along the United States eastern continental margin. BMC. Res. Notes 17. https://doi.org/10.1186/s13104-024-06977-4.
Whiting, M.F., Carpenter, J.C., Wheeler, Q.D., Wheeler, W.C., 1997. The Strepsiptera Problem: Phylogeny of the Holometabolous Insect orders Inferred from 18S and 28S Ribosomal DNA Sequences and Morphology. Syst. Biol. 46, 1–68.
Wilson, J.B., 1979. The distribution of the Coral *Lophelia pertusa* [L. prolifera (Pallas)] in the North-East Atlantic. Journal of the Marine Biological Association of the United Kingdom 149–164.

Winsnes, I.M., 1989. Eunicid polychaetes (Annelida) from scandinavian and adjacent waters. Family Eunicidae. Zool Scr 18, 483–500.

Xu, T., Sun, J., Lv, J., Kayama Watanabe, H., Li, T., Zou, W., Rouse, G.W., Wang, S., Qian, P.Y., Bao, Z., Qiu, J.W., 2017. Genome-wide discovery of single nucleotide polymorphisms (SNPs) and single nucleotide variants (SNVs) in deep-sea mussels: potential use in population genomics and cross-species application. Deep Sea Res 2 Top Stud Oceanogr 137, 318–326. https://doi.org/10.1016/j.dsr2.2016.03.011.

Zanol, J., Carrera-Parra, L.F., Steiner, T.M., Amaral, A.C.Z., Wiklund, H., Ravara, A., Budaeva, N., 2021. The current state of eunicida (Annelida) systematics and biodiversity. Diversity (basel) 13, 1–54. https://doi.org/10.3390/d13020074.

Zanol, J., Halanych, K.M., Fauchald, K., 2014. Reconciling taxonomy and phylogeny in the bristleworm family Eunicidae (polychaete, Annelida). Zool. Scr. 43, 79–100. https://doi.org/10.1111/zsc.12034.

Zanol, J., Halanych, K.M., Struck, T.H., Fauchald, K., 2010. Phylogeny of the bristle worm family Eunicidae (Eunicida, Annelida) and the phylogenetic utility of noncongruent 16S, COI and 18S in combined analyses. Mol. Phylogenet. Evol. 55, 660–676. https://doi.org/10.1016/j.ympev.2009.12.024.

Zanol, J., Hutchings, P.A., Fauchald, K., 2020. Eunice sensu latu (Annelida: Eunicidae) from Australia: Description of seven new species and comments on previously reported species of the genera Eunice, Leodice and Nicidion. Zootaxa 4748, 1–43. https://doi.org/10.11646/zootaxa.4748.1.1.

Zanol, J., Paiva, P.C., Attolini, F.D., 2000. Eunice and Palola (Eunicidae: Polychaeta) from the eastern Brazilian Coast (13°00'-22°30'S). Bull. Mar. Sci. 67, 449–464.